Multimodality Imaging of Carotid Atherosclerotic Plaques:

Comparison of Contrast Enhanced USG, CT and MRI

THESIS

SUBMITTED IN PARTIAL FULFILLMENT FOR DEGREE OF

DM (NEUROIMAGING AND INTERVENTIONAL NEURORADIOLOGY)

(2010-2012)

OF THE

SREE CHITRA TIRUNAL INSTITUTE FOR MEDICAL SCIENCES AND TECHNOLOGY, TRIVANDRUM, INDIA

Dr. Divyata Rajendra Hingwala

Department of Imaging Sciences & Interventional Radiology,

SREE CHITRA TIRUNAL INSTITUTE FOR MEDICAL SCIENCES AND TECHNOLOGY

TRIVANDRUM, INDIA

DECLARATION

I hereby declare that this thesis entitled '**Multimodality Imaging of Carotid Atherosclerotic Plaques**: **Comparison of Contrast Enhanced USG, CT and MRI'** has been prepared by me under the supervision and guidance of **Dr. C. Kesavadas**, Professor, Department of Imaging Sciences and Interventional Radiology, Sree Chitra Institute for Medical Sciences and Technology, Thiruvananthpuram.

Date:

Place: Trivandrum

Dr. Divyata Rajendra Hingwala

DM Neuroimaging and Interventional Neuroradiology Resident, Department of Imaging Sciences and Interventional Radiology, SCTIMST, Trivandrum.

SREE CHITRA TIRUNAL INSTITUTE FOR MEDICAL SCIENCES AND TECHNOLOGY, TRIVANDRUM

CERTIFICATE

This is to certify that the work incorporated in this thesis entitled '**Multimodality Imaging of Carotid Atherosclerotic Plaques**: **Comparison of Contrast Enhanced USG, CT and MRI'** for the degree for **DM (NEUROIMAGING AND INTERVENTIONAL NEURORADIOLOGY)** has been carried out by **Dr. Divyata Rajendra Hingwala** under my supervision and guidance. The work done in connection with this thesis has been carried out by the candidate herself and is genuine.

Dr Kapilamoorthy TR
Professor and Head

Dr C Kesavadas
Professor
Guide

Department of Imaging Sceinces and Interventional Radiology

ACKNOWLEDGEMENTS

I am deeply indebted to my honorable teacher and guide **Dr C. Kesavadas** (Professor, Dept. of Imaging & Interventional Radiology) for his constant support, encouragement, helpful criticism, expert supervision and guidance throughout this study which assisted largely in bringing this study to fruition.

I wish to thank Dr. Kapilamoorthy T R (Professor & HOD), for spending his valuable time to go through our work in detail and giving positive suggestions and encouragement.

I am also profoundly grateful to Dr A K Gupta, Dr. Bejoy Thomas , Dr. Narendra Bodhey, Dr. Hima S Pendharkar, Dr Jayadevan ER and Dr. Santhosh Kannath for lending instant support whenever needed.

I would like to thank the institute for funding this research as a 'student project' and Dr Sylaja PN, Additional Professor (In- Charge of Comprehensive Stroke care program) and Dr Unnikrishnan M, Professor and Head, Department of Vacular Surgery for their support with this project. I am also grateful to Dr P Sankara Sarma and Dr Jissa TV, Department of Biostatistics Achuta Menon Center for Health Sciences, for their invaluable help with the statistical analysis.

I would like to acknowledge my gratitude to my seniors and all my co-residents for their valuable guidance & constant support.

I would also like to extend my special gratitude to all technologists and Diploma in Advanced Medical Imaging Technology students and the entire department staff for making all the scans possible.

Last but most important; I am grateful to all my patients and their relatives who have been so co-operative despite their own sufferings & agreed to become the part of this study.

Dr. Divyata Rajendra Hingwala
Senior Resident,
Dept of IS & IR,
SCTISMT, Thiruvananthapuram,
India.

INDEX

SECTIONS	PAGE NUMBER
Introduction	6
Aims and objectives	7
Review of literature	8
Material and Methods	26
Results	37
Representative cases	50
Discussion	56
Conclusion	66
References	67
Annexures	
Proforma	83
Technical Advisory committee approval letter	84
Institutional Ethics committee approval letter	85
Grant approval letter	86
Masterchart	87

Introduction

Stroke is one of the most important causes of death and the greatest cause of disability all over the world. Approximately 20% to 30% of the infarcts can be related to carotid artery stenosis.[1] The severity of stenosis is a standard parameter in the evaluation of risk, and it is one of the most important criteria that may influence the choice of treatment. However, it is possible that even a low-grade stenosis in the carotid arteries can lead to the development of cerebrovascular events. Hence, it may be important to look beyond the degree of stenosis and determine wall and plaque morphology. Besides the severity of stenosis, other factors like plaque ulceration, composition and neovascularization are independent predictors of stroke.

While previously only the degree of carotid stenosis was used to determine treatment options in patients with carotid plaques, now there is a paradigm shift with increasing importance being given to plaque characterization to determine which patients would benefit from surgical treatment. Patients with 'vulnerable' plaques are more prone to developing future neurovascular events. Neovascularization is an important factor contributing to vulnerability of atherosclerotic plaque.

We hypothesized that certain morphologic characteristics of atherosclerotic plaque could serve as an adjunct to stenosis grade and that multimodality imaging may provide additional information that could help in risk stratification of patients with carotid plaques .

Aims and Objectives

The purpose of this study is

- To describe the methodology and technical aspects of contrast enhanced ultrasound, CTA and MRI in the evaluation of carotid plaques
- To study the role of these techniques in the assessment of carotid atherosclerotic plaques and discuss the related clinical implications

Review of Literature

Significance of detecting vulnerable plaques

The concept of 'plaque vulnerability' was first introduced in the context of coronary arteries.[2] Consensus statements[3,4] published by a group of experienced researchers in atherosclerosis, including pathologists, clinicians, molecular biologists, and imaging scientists have elaborated on the key features of the vulnerable plaque were defined. These documents state that knowledge of luminal diameter is not sufficient to determine the vulnerability of an atherosclerotic lesion, and they propose five major and five minor criteria for the detection of vulnerable plaques.

Golledge[5] et al performed a metaanalysis of the histologic studies of carotid plaques. According to them, there are 2 types of carotid artery disease: one form stable and unlikely to produce symptomatic embolization or carotid occlusion and a second form, while not necessarily being any more stenotic, unstable and at high risk of producing symptomatic embolization or carotid occlusion.[5] Majority of ischemic strokes appear to result from embolization from an atherosclerotic plaque or acute occlusion of the carotid artery and propagation of thrombus distally.[5] The frequency of embolization on transcranial Doppler (TCD) is greater in patients with recent symptoms such as transient ischemic attack (TIA) compared with patients with similarly severe asymptomatic disease.[6]

Fibrous cap

Redgrave et al[7] performed histological measurements of fibrous caps. They found that critical cap thickness is greater in carotid plaques than coronary plaques. Minimum and representative cap thicknesses were both independently associated with cap rupture. A

combination of minimum cap thickness <200 microns and a representative cap thickness <500 microns identified ruptured plaques most reliably. Prospective imaging studies are required to establish whether these cut points predict clinical events in patients with asymptomatic carotid stenosis.

Physiology of vasa vasorum

The vasa vasorum[8] form a network of microvasculature that originates primarily in the adventitial layer of large arteries [vasa vasorum externa (VVE)] with the function of supplying oxygen and nutrients to the outer layers of the arterial wall. In larger mammals, the vasa vasorum can also originate from the luminal surface [vasa vasorum interna (VVI)] or from the media. Additionally, there are the venous vasa vasorum (VVV) that drain the arterial wall in companion veins.[9]

As atherosclerosis progresses, there is a thickening of the intima-media complex exceeding the oxygen diffusion threshold (250 to 500 microns), inducing ischemia, which then triggers a continual release of angiogenic growth factors (vascular endothelial growth factor, tissue hypoxic factor, and so on). [10] It is believed that the absence of pericytes in some angiogenic vessels causes these immature vessels to "leak" potentially noxious and inflammatory plasma components (hemoglobin, oxidized low-density lipoprotein cholesterol, lipoprotein[a], glucose, advanced glycation end products, and inflammatory cells) into the extracellular matrix of the media/intima, increasing plaque volume. The ongoing deposit of plasma components appears to further reduce vessel wall oxygen diffusion, triggering continued growth of angiogenesis. Ultimately, the plaque is enveloped in luxurious adventitial vasa vasorum and intraplaque neovascularization, a hallmark of symptomatic atherosclerosis.[11]

The presence and extent of vasa vasorum correlate with atherosclerotic lesion size and lumen diameter in hypercholesterolemic mouse models.[12-14]

Several pathological studies showed that a more extensive plaque neovascularization is associated with features of plaque vulnerability and with clinically symptomatic disease.[15-17] Histopathologic studies have confirmed plaque neovascularization as a consistent feature of vulnerable plaque in patients with cerebrovascular disease.[15,18] The relationship between histological aspects of carotid plaque vascularisation and cerebral symptoms has been described by ***McCarty*** et al[17], who identified a higher number of microvessels in symptomatic plaques.

Dunmore et al[18]. similarly showed this correspondence and identified a relationship between cerebral symptoms and the carotid plaque vessel morphology; irregular dysmorphic vessels were found almost exclusively in plaques from symptomatic patients.

Mofidi et al[19] have observed a significantly higher microvessel counts in patients with CT evidence of ipsilateral cerebral infarction.

Plaque ulceration

The presence of ulceration in the carotid plaque significantly increases the risk of cerebrovascular events[20-21]Varying incidences of ulcerations on carotid plaques have been described. ***Lovett*** et al[22] have reported a prevalence of ulceration of 14% based on the DSA data of the ECST study. ***Eliasziw*** et al[23] found ulcerations in 35% of the symptomatic arteries in the NASCET study.

The Oxford plaque study[7] was a histological study of symptomatic carotid endarterectomy specimens from 526 consecutive patients with a stenosis degree of 75% to 90%. Ulceration was found in 58% of the specimens. Golledge et al[5] found that ulceration was more common in symptomatic than in asymptomatic plaques (48% versus 31%, P<0.001),but lumen thrombus and intraplaque hemorrhage were equally prevalent in both groups. In symptomatic patients the necrotic core is placed nearer to the fibrous cap and the minimum cap thickness is less.

The accuracy of digital subtraction angiography (DSA) in the detection of ulceration, with surgical observations as reference, has been reported to be low (sensitivity 46% and specificity 74%).[24] Oliver et al reported the first study on the accuracy of CT angiography (CTA) compared with DSA in the assessment of plaque ulcers. The results of CTA were disappointing, but this might be explained by the rather thick slice thickness used with single-section CT.[25] ***Randoux*** et al[26] later reported that CTA was superior to DSA in the detection of plaque irregularities and ulcerations. ***Saba*** et al[27] also reported a high sensitivity and specificity for the detection of ulcerations (94% and 99%, respectively).

CT angiogram

Lovett et al[28] characterized ulcerations as Type 1 to 4 based on the location of the ulcer neck and ulcer orientation [Circ 2004]. Type 1 is an ulcer that points out perpendicular to the lumen; Type 2 has a narrow neck and points out proximally and distally; Type 3 has an ulcer neck proximally and points out distally, and Type 4 has an ulcer neck distally and points out proximally.

Lovett et al[22] reported a prevalence of ulceration of 14% in 3007 symptomatic carotid arteries in patients with TIA or minor stroke, and a prevalence of 18% for symptomatic carotid arteries with a stenosis > 30%.

In a recently published study, ***Saba*** et al[29] assessed carotid artery plaque volume and composition and the presence of ulceration on MDCTA. They found no correlation between total carotid atherosclerotic plaque volume and ulcerations, whereas plaque relative lipid volume (using attenuation of < 60 HU) was associated with the presence of ulceration. On ROC curve threshold analysis, the best threshold for the association with ulceration in the plaque was 270 mm^3 of fatty components, with sensitivity of 75% and specificity of 82%. They also found that hypertension was significantly associated with the presence of ulcerations.

Besides MDCTA and DSA, MR angiography has been used for the assessment of atherosclerotic carotid plaque surface morphology. ***Randoux*** et al[26] made a comparison between these techniques and concluded that luminal surface irregularities were most frequently seen at CTA and that with CTA and MR angiography, more ulcerations were detected than with DSA.

Saba et al[27] have recently showed that ultrasound has a high specificity (93%) but a low sensitivity (38%) for the detection of carotid ulceration.

Homburg et al[30] found that plaque volume was significantly greater in ulcerated plaques.

Saba et al[21] investigated the relationship between degree of stenosis, symptoms, plaque type on CT angiogram, and presence of CT-detectable brain lesions. On simple logistic regression there was a statistically significant positive association between fatty plaque

type and symptoms ($p < 0.001$) and between >70% stenosis and symptoms ($p = 0.041$). Moreover, an inverse association was observed between calcified plaques and symptoms ($p = 0.009$ with regression r coefficient - 1.398).

The study by ***deWeert*** et al[31] showed that MDCTA can classify atherosclerotic carotid plaque surface morphology. The presence of a complicated plaque surface in an atherosclerotic plaque is strongly related with the severity of stenosis and that the site of ulceration is mostly proximal to the most stenotic site. In addition, it is shown that hypercholesterolemia and probably smoking are related to the presence of complicated plaques. It was also shown that complicated plaque is more common in the symptomatic artery of patients with cerebrovascular symptomatology than in the asymptomatic artery.

Ultrasound assessment of carotid plaques

Echogenicity on ultrasound has been shown to predict ipsilateral ischaemic stroke; patients with echolucent plaques are at increased risk compared to those with echorich plaques.[32,33] However, hazard ratios for development of stroke that are associated with differing echogenicity scores are not sufficiently great to warrant translation into clinical practice. Furthermore, studies investigating the use of GSM in selection for carotid artery stenting (CAS) have had conflicting results. The Imaging in Carotid Angioplasty and Risk of Stroke (ICAROS) study[34] revealed that high echolucency increases risk of stroke as a complication of CAS. Subsequently, ***Reiter*** and colleagues[35] showed no such relationship between plaque echolucency and stroke risk with CAS.

Swijndregt[36] reported difficulty in reliably identifying the near wall of the carotid vessel in vitro using extravascular ultrasound techniques

Wong et al[37] reported that conventional ultrasound, without contrast, routinely underestimated near wall c-IMT thickness by 20%.

Contrast enhanced ultrasound of carotid plaques

The first studies of contrast enhanced ultrasound for the evaluation of carotid plaque neovascularization were performed by ***Feinstein*** et al[10]. They showed a moderate correlation coefficient of 0.64.

Several other authors have described the possibility of identifying carotid plaque neovascularization in vivo.

Coli et al[38] found that plaques with higher contrast-agent enhancement showed a greater neovascularization at histology (grade 2 vs. grade 1 contrast-agent enhancement: median vasa vasorum density: 3.24/mm2 vs. 1.82/mm2, respectively, p = 0.005). In the whole series of 52 lesions, echolucent plaques showed a higher degree of contrast-agent enhancement (p <0.001). Stenosis degree was not associated with neovascularization at histology or with the grade of contrast-agent enhancement. They concluded that carotid plaque contrast-agent enhancement with sonographic agents correlates with histological density of neovessels and, therefore, is a promising tool to study plaque vasa vasorum in the clinical setting

Saha et al[39] compared semiquantitatively CEUS with histological characteristics. Their findings revealed that contrast enhancement within the plaque is correlated with higher number of microvessels.

Giannoni et al[40] reported diffuse contrast uptake in plaques from symptomatic patients,51 all of whom had increased number of microvessels confirmed on histology.

The latter group described the common presence of small vessels within plaque underlying ulcerations.

The study by ***Fagglioli*** et al[41] revealed that plaques with elevated number of microvessels and high vessel total area showed a significantly higher contrast enhancement at CEUS software evaluation. A significantly higher dB-E (Decibel enhancement) was found in plaques with thin fibrous cap and elevated inflammatory infiltrate. They also observed a direct correlation between CEUS characteristics of the carotid plaque and cerebral symptoms. Similarly, clinical symptoms and CT scan signs of cerebral infarction are correlated with higher levels of dB-E at CEUS evaluation. Specifically, patients with positive cerebral CT scan had significantly higher plaque dB-E than patients with negative CT; thus, CEUS may help in the identification of plaques with higher embolic potential.

Xiong and colleagues[42] studied 104 carotid stenoses using time-signal intensity curves with automated image analysis. Their study revealed that plaque enhanced intensity and the intensity normalized against carotid luminal intensity were both significantly greater in symptomatic versus asymptomatic atheromata.

A preliminary study by ***Hoogi*** et al[43] studied quantification of neovascularization on contrast enhanced ultrasound using a computerized method in patients with severe carotid stenosis (>70%). Definity contrast medium was used. Continuous cine loops were recorded. Motion compensation and synchronization with the cardiac cycle was performed for image coregistration. Segmentation of the contrast-enhanced regions within the plaque in each frame was also performed by the Chan and Vese method. They found that quantification of neovessels using contrast-enhanced ultrasound of the

plaque was well correlated with the histologic results regarding the area of neovascularization (R2 = 0.7905) and with the number of inflammatory cells present in the plaque (R2 = 0.6109). The calculated p values supported these results and showed significant dependence between the examined features ($p < 0.01$).

Moreno and Fuster[44] have directly linked atherosclerosis and diabetes to the formation of vulnerable plaque. ***Mauriello*** et al[45] examined 544 coronary segments in 16 patients who experienced fatal coronary events. The results revealed the presence of diffuse, active inflammation in the entire coronary vascular system, in patients with both stable and vulnerable plaques.

Owen et al[46] assessed carotid plaque inflammation using delayed enhancement on ultrasound. By quantifying microbubble retention within the carotid plaque, late phase contrast-enhanced US depicts clear differences between groups of subjects with plaque ipsilateral to symptoms and asymptomatic plaques. This technique has promise as a tissue-specific marker of inflammation and a potential role in the risk stratification of atherosclerotic carotid stenosis.

Using animal models with dietary-induced atherosclerosis, ***Williams*** et al[47] showed regression of intima and media neovascularization after a reduction of cholesterol feeding.

Moulton et al[48] studied antiangiogenesis therapies in an experimental animal model of atherosclerosis.

Ultrasound contrast medium

Microbubble-based contrast agents are injected intravenously to enhance ultrasound scans, and are composed of 1-10 mm diameter albumin or lipid shells filled with air or high molecular weight gas. Their small size allows them to recirculate, whereas larger bubbles are retained in the pulmonary circulation.

The discovery that gas filled bubbles can act as ultrasound contrast agents was initially made because the density change from blood to intrabubble gas causes reflection of sound waves.[49] However, modern ultrasonic methods of distinguishing microbubble from native tissue rely on the fact that ultrasound waves cause microbubbles to compress and expand, whereas tissue is virtually incompressible. By fortunate coincidence, the resonance frequency for microbubbles (the frequency at which compression and expansion occurs most readily) is within the range of frequencies used for clinical ultrasound. Sound waves of very low energy, therefore, will return detectable signal from microbubbles, provided the transmitted wave is around the microbubble resonance frequency. Native tissue, however, will not respond to such low energy waves.[50] (**Figure 1**).

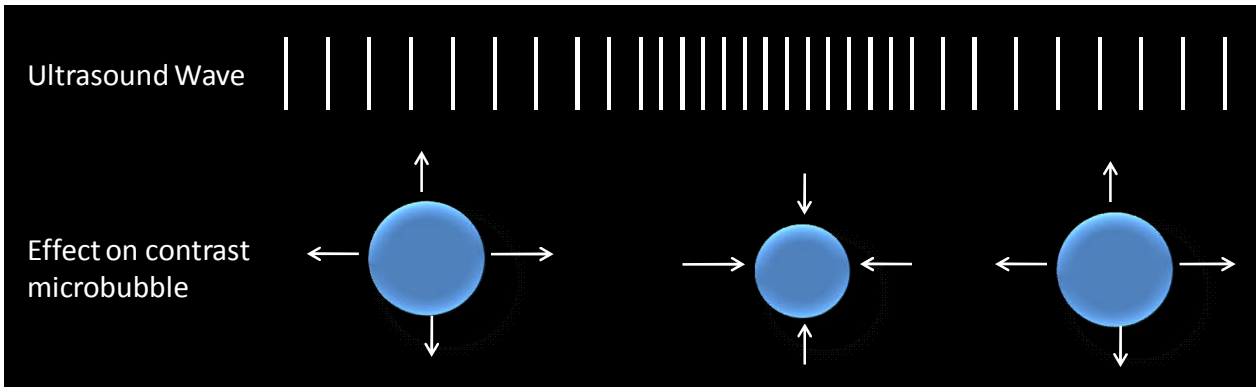

Figure 1: Mechanism of action of ultrasound contrast agents

Unlike most contrast agents used for CT and MRI, microbubbles remain within the vascular space and are hence well suited to study the vasculature. By improving visualization of the lumen, contrast enhanced ultrasound (CEUS) can improve current carotid structural scans. Furthermore, CEUS may be able to add extra information on plaque characteristics, such as neovascularisation, deemed to elucidate plaque instability. In addition, manufacturing microbubbles targeted to specific vascular endothelial ligands, CEUS may have the ability to probe plaque biology.

Sonovue, Bracco, Italy is a suspension of phospholipid stabilized sulphur hexafluoride (SF_6) microbubbles . It is a second generation of ultrasound contrast agent.

When reconstituted with normal saline the product is stable at room temperature for several days, but should be used after reconstitution within 6 h as the product contains no preservative. Reconstitution produces a high microbubble concentration (upto 5 x 10^8 microbubbles /ml). The microbubbles produced have favourable size characteristics (90% of microbubbles smaller than 8.0 mic, mean diameter 2.5 mic). The microbubbles produced are not trapped in the capillary vasculature

Use of SF_6 (an innocuous gas) renders the microbubbles more resistant to pressure increases from the left ventricle of the heart, increasing microbubble survival . SonoVue demonstrates a maximum backscatter coefficient at about 3 MHz. Elimination half-life is approximately 6 min. More than 80% of the compound is exhaled via the lungs in 11 min.

MRI plaque imaging

Noninvasive MR imaging has great potential to help characterize atherosclerotic plaque composition[51] and morphology and thus to enable assessment of plaque vulnerability. Naghavi et al[2] have given 5 major and 5 minor criteria of vulerable plaques.

Virmani et al[52] defined the fibrous cap as a distinct layer of connective tissue completely covering the lipid-necrotic core.

Yuan et al[53] found that the presence of a thin or ruptured FC, as seen on magnetic resonance imaging (MRI) scans was highly associated with recent TIA or stroke. Similarly, Saam et al. [Radiology 2006] found a much higher incidence of FC rupture was found in symptomatic patients than in asymptomatic patients (78% vs. 30%, respectively).

An ex vivo imaging study by ***Shinar*** et al[54] demonstrated that tissue components, including the lipid-necrotic core, hemorrhage, and calcification, could be detected with sensitivities and specificities ranging from 84% to 100%. ***Yuan*** et al[55] performed an in vivo imaging and showed that the lipid-necrotic core and intraplaque hemorrhage could be identified with a high sensitivity of 85% and a specificity of 92% . ***Cai*** et al[56] showed that in vivo MR imaging can help identify sections that have either a lesion with a confluent extracellular lipid-necrotic core (American Heart Association type IV lesion) or a lipid-necrotic core covered by a fibrous cap (type V lesion), with a sensitivity of 84% and a specificity of 90%. ***Clarke*** et al[57] intitially attempted quantification of various components of plaques, who used diffusion-weighted imaging in addition to T1-, intermediate-, and T2- weighted imaging, pixels were classified into different plaque components and were then compared with histologic specimens.

Saam et al[58] evaluated the ability of MRI to quantify all major carotid atherosclerotic plaque components in vivo compared with histopathology. MRI measurements of plaque composition were statistically equivalent to those of histology for the LR/NC (23.7 versus 20.3%; P_0.1), loose matrix (5.1 versus 6.3%; P=0.1), and dense (fibrous) tissue (66.3% versus 64%; P=0.4). Calcification differed significantly when measured as a percentage of wall area (9.4 versus 5%;P < 0.001). Intrareader and inter-reader reproducibility was good to excellent for all tissue components, with ICCs ranging from 0.73 to 0.95.

MR measurements of the lipid necrotic core did not differ significantly from findings on histologic specimens (23.7% vs 20.3%; P < .1), and a strong correlation between MR and histologic area measurements was found (r =0.75; P < .001). [58]

Cai et al[59] concluded that in vivo high-resolution CEMRI is capable of quantitatively measuring the dimensions of the intact FC and LR-NC and has good correlation with histopathology.

Sakamoto et al[60] found that a carotid stenotic lesion with a vulnerable plaque found by MR plaque imaging (especially one with intraplaque hemorrhage) has a significantly higher risk of the slow-flow phenomenon in CAS than lesions with other plaque compositions. The occurrence of the slow-flow phenomenon during carotid angioplasty and stenting, which may increase the risk of complications, can be predicted and reduced by considering the information about plaque composition indicated by MR plaque imaging.

Intraplaque hemorrhage is an important mechanism for carotid atherosclerotic plaque progression.

Yuan et al[61] have shown that MRI can detect carotid lipid-rich necrotic cores and intraplaque hemorrhage with good accuracy.

Chu et al[62] grouped hemorrhage into fresh, recent, and old categories using a modified MRI cerebral hemorrhage criteria and compared with histopathology. Hemorrhage was histologically identified and staged in 145/189 (77%) of carotid artery plaque locations. Acute and recent hemorrhage both had hyperintense signal on T1WI and TOF source images. However, T2W and PD hyperintensity distinguishes recent from fresh hemorrhage. Chronic hemorrhage has variable hypointensity on all sequences. MRI detected intraplaque hemorrhage with high sensitivity (90%) but moderate specificity (74%). Moderate agreement in classifying stages occurred between MRI and histology.

Kampschulte et al[63] studied the role of MRI in distinguishing between intraplaque and juxtaluminal thrombus. The sensitivity and specificity for MRI to correctly identify cross sections that contained hemorrhage were 96% and 82%, respectively. Furthermore, MRI was able to distinguish juxtaluminal hemorrhage/thrombus from intraplaque hemorrhage with an accuracy of 96%. The distribution of lesion types underlying hemorrhages differed significantly (P=0.004). Intraplaque hemorrhage had an underlying lipid-rich type IV/V lesion in 55% of histological sections, whereas juxtaluminal hemorrhage/thrombus had an underlying calcified lesion type VII in 70% of sections.

Ota et al[64] compared the diagnostic performances of three T1-weighted 3.0-T magnetic resonance (MR) sequences at carotid intraplaque hemorrhage (IPH) imaging, with histologic analysis as the reference standard. These included two-dimensional fast spin-echo, three-dimensional time-of-flight (TOF), and three-dimensional magnetization-

prepared rapid acquisition gradient-echo (RAGE) sequences. The magnetization-prepared RAGE sequence, as compared with the fast spin-echo and TOF sequences, demonstrated higher diagnostic capability for the detection and quantification of IPH. However, these sequences cannot be used reliably to detect small IPHs or IPH mixed with heavy calcification. As compared with imaging at 1.5T, this study indicated higher specificity and similar or better agreement.

Murphy et al[65] have demonstrated that a T1-weighted (T1W) magnetization prepared three-dimensional (3D) gradient echo sequence can detect methemoglobin within intraplaque hemorrhage.

Altaf et al[66] found that plaque hemorrhage seen at MR imaging helps predict microembolization during the dissection phase of carotid endarterectomy.

Altaf et al[67] studied the association of plaque hemorrhage on MRI with thromboembolic activity. In patients with carotid plaque hemorrhage demonstrated at MR imaging (T1-weighted gradient-echo fat-suppressed sequence), there was increased spontaneous microembolic activity at transcranial doppler imaging and cerebral ischemic lesion patterns suggestive of recurrent embolic events. Ipsilateral diffusion abnormalities were seen in 12 of 32 [38%] patients with plaque hemorrhage versus none of 19 patients without plaque hemorrhage; P<, .05 (odds ratio, 6.2 [95% confidence interval: 1.7, 21.8]; P < .05). The presence of plaque hemorrhage also increased the presence of microembolic signal (odds ratio, 6.0 [95% confidence interval: 1.8, 19.9]; P = .003). These findings suggest that plaque hemorrhage shown at MR imaging might be a marker of thromboembolic activity and further validate the usefulness of carotid imaging in identifying patients with active carotid arterial disease.

According to ***Yuan*** et al[53], three dimensional TOF native sections, based on a gradient-echo sequence with a low flip angle, show the hyperintense lumen, the soft tissue, and the fibrous cap.

Hatsukami et al[68] were able to characterize the state of the fibrous cap as being (a) intact and thick, (b) intact and thin, or (c) ruptured. They hypothesized that this was due to the lamellar nature of the fibrous cap. Serfaty et al showed that the fibrous cap can also be seen on T2-weighted images and with short inversion time inversion-recovery (STIR) sequences as a hyperintensity located between the dark lumen and the plaque.

Mitsumori et al[69] compared histologic findings with preoperative MR imaging appearance of the fibrous cap. MRI has a high test sensitivity (0.81) and specificity (0.90) for identifying an unstable cap in vivo. However, confounding causes of hypointense signal in the plaque mimicking plaque rupture include juxtaluminal calcification and chronic hemorrhage.[70]

Apart from routine fse T1, T2 and PD sequences, alternative contrast agents can be used. ***Raman*** et al[71] found a significant reduction of T2* in symptom-causing plaques, which was attributed to higher amounts of T2*-shortening forms of iron.

Zhu et al[72] introduced a novel imaging technique (3-dimensional [3D] SHINE) to combine T1-weighted spoiled gradient inversion recovery imaging to detect intraplaque hemorrhage with multi-echo measurement of T2* to stage the hemorrhage in hemoglobin byproducts.

Yang[73] applied SWI in femoral arteries.

Ultrashort echo time (UTE) imaging techniques have been introduced to obtain signal from species with T2 values well under 1 ms (like lipoproteins and collagen) using specialized slice selection techniques and radial k-space trajectories.[74]

Magnetization transfer is another means of imaging species with ultrashort T2 values.[75]

Toussaint et al[76] and ***Clarke*** et al[77] have shown that necrotic core regions of plaque have significantly lower diffusion coefficients and higher DWI intensities than fibrous regions.

Kerwin et al[78] used this approach to construct 'vasa vasorum images' that color code plaque regions according to the estimated vp and Ktrans

In addition to plaque composition, MRI can also be used to study plaque progression. ***Saam*** et al [79] showed a mean wall area increase of 2.2%/year and a mean luminal area decrease of 1.9%/year. In this study, the disease progression was about four times greater in patients who were not treated with statins compared with patients who were treated. A normalized wall index (NWI=wall area/total vessel area) >0.64 (P=0.001) was associated with a significantly reduced rate of progression in mean wall area. ***Corti*** et al[80] demonstrated a decrease in plaque burden after 2 years of therapy with simvastatin.

Plaque inflammation

Wasserman et al[81] showed that the wash-in kinetics of gadolinium into the fibrous cap and lipid core may be correlated with the degree of neovascularization. Other techniques for detecting plaque inflammation include the use of USPIO nanoparticles.[82]

For carotid imaging with a 1.5-T MRI scanner, echo-planar capabilities are advantageous because the gradient amplifiers and higher slew rates supported by these systems allow shorter echo times and echo spacing (in fast SE sequences).

The carotid arteries are superficial structures whose length is greater than their distance from the surface. This configuration is well suited for the use of phased array surface coils, which are composed of several adjacent small surface coils that collect data simultaneously. For the purposes of carotid plaque imaging, a dedicated phased-array coil assembly (Figure 3) with overall dimensions of 6.4 x 10.8 cm was used. The assembly consists of two separate sets of coils to allow imaging of both carotid arteries during an examination. Each coil is made of a soft flexible material that can be comfortably fitted and secured about the patient's neck. With this coil assembly, an effective longitudinal coverage of up to 5 cm can be achieved. Studies of the performance of these phased-array coils in healthy volunteers demonstrated a 37% improvement in the signal-to-noise ratio.

Figure 2: Carotid surface coils

Material and Methods

Study design

We performed a prospective study to compare the enhancement characteristics of carotid atherosclerotic plaques on contrast enhanced ultrasound and CT and MRI plaque morphology and correlate this with the patients' clinical symptoms. This multimodality observational study compared various imaging modalities for carotid atherosclerotic plaque characterization.

Study location and duration

This study was performed at our institute which is a tertiary referral center in South India with a 'Comprehensive stroke care' unit. It was performed over a period of 20 months from November 2010 to June 2012.

Study Population

Consecutive patients (n=24) with 50 to 99% stenosis by sonography or CT angiography (NASCET criteria) underwent carotid plaque imaging with contrast enhanced ultrasound, CTA and high resolution MRI.

26 patients were prospectively studied. Patients who had ischemic cerebrovascular disease, including amaurosis fugax or focal cerebral ischemia (TIA and minor ischemic stroke were recruited from the neurology department's specialized stroke outpatient clinic or stroke ward. Carotid Doppler was also performed to study the arteries of asymptomatic patients who underwent cardiac interventions for coronary artery disease, aortic interventions, and lower leg artery surgery and for patients with diabetes who were older than 50 years.

Patients were prospectively enrolled. Patients underwent multidetector CTA, ultrasound, contrast enhanced ultrasound and high resolution MRI of the carotid arteries with special emphasis on the carotid bifurcation. The study protocol was approved by the technical advisory committee and the Institutional Review Board (Anneures). This research was conducted in accordance with the guidelines of our Institutional Review Board. All patients gave written informed consent. The study was an institute funded student project. The funding body did not pay any role in study design, data collection, analysis or reporting of this study.

Selection criteria

Inclusion criteria

Patients with an ultrasound examination that showed a stenosis (50% stenosis according to the NASCET criteria or a plaque were explained about the study. Patients were included if they were willing to provide consent to participate in this study, age > 40 years, renal function was normal (serum creatinine <1.2mg/dl)and they had greater than 50 % stenosis on B mode ultrasound according to NASCET criteria

Exclusion criteria

A known allergy to the iodinated contrast material, elevated renal function test results and cardiac failure excluded the patients from undergoing CTA.

Patients were questioned regarding their history of drug allergy, asthma, chronic lung disease, and right-to-left cardiac shunt, which are contraindications to the administration of the ultrasound contrast agent [Hoogi, AJR]. Patients with plaque calcification

involving greater than 30% of plaque area were also excluded (as calcification would preclude assessment of contrast enhancement on ultrasound.

Contraindications to MRI examinations included pacemakers, metallic implants, claustrophobia.

Patients who were not interested in participation/ did not give informed consent or those who clinically required emergent surgery (endarterectomy) were also excluded from this study.

Cardiovascular Risk Factors

Medical history was recorded from all patients. Patients underwent neurological examination on admission. Clinical measures and information on risk factors and medication were obtained at admission to the hospital or from our medical records department. Diabetes, hypertension, smoking, dyslipidemia. Information on previous cardiovascular disease (myocardial infarction, atrial fibrillation, angina pectoris, chronic heart failure, coronary artery bypass grafting) and previous ischemic cerebrovascular disease (TIA or ischemic stroke other than the event for which the patient was currently evaluated) was collected.

Subjects were categorized as current, past, and never smokers. Hypertension was defined as systolic blood pressure over 140 mm Hg and/or diastolic blood pressure over 90 mm Hg or treatment with antihypertensive medication. Hypercholesterolemia was defined as fasting cholesterol_5.0 mmol/L or on treatment with cholesterol-lowering drugs. Diabetes was defined as fasting serum glucose levels >7.9 mmol/L, nonfasting serum glucose levels >11.0 mmol/L, or use of antidiabetic medication.

Symptoms

Amaurosis fugax was defined as a sudden, focal neurological deficit that was presumed to be of vascular origin and confined to the eye.

TIA was defined as a sudden, focal neurological deficit that was presumed to be of vascular origin and was confined to an area of the brain perfused by a specific artery and that lasted then 1 hour. In addition, no relevant infarct (one that explains the deficit) should be seen on the CT scan.

An ischemic stroke was defined as a sudden focal neurological deficit that lasted more than 1 hour or which was accompanied by a relevant infarct on the CT scan.

Imaging technique

B mode ultrasound

Ultrasound carotid duplex scanning was performed with a Phillips iU22, with standard vascular presets, and equipped with contrast multipulse nonharmonic imaging software CPS. Linear phased array probes (7 and 12 MHz) with standard presettings were used to assess carotid plaques. The same machine presets were maintained for all the patients.

Linear probes of 7 and 12 MHz were used for standard duplex, according to a routine protocol used for all patients in our institute, and comprising the recordings of (a) the B mode, color and power mode evaluation of the common carotid artery, the bulb, the proximal and distal internal carotid and the external carotid arteries, to exactly evaluate plaque morphology both in longitudinal as well as in transverse axes; (b) the pulsed-wave Doppler evaluation of blood flow velocities in the proximal common carotid, in

the internal carotid at the prestenotic segment, at the point of maximum stenosis and at the poststenotic segment, and in the external carotid arteries.

Contrast enhanced ultrasound

Contrast reconstitution

Sonovue is supplied in a plastic jacket which contains a glass syringe prefilled with normal saline (0.9% w/v NaCl), a plastic plunger, a MiniSpike transfer system and a vial containing 25 mg of dry, lyophilized powder in an atmosphere of sulphur hexafluoride.

The contents of the prefilled syringe (0.9% w/v NaCl) are transferred to the vial using the MiniSpike transfer system Sulphur hexafluoride powder. The vial is shaken vigorously for 20 seconds to mix contents. On reconstitution, 1 ml of the resulting dispersion contains 8 microlitres sulphur hexafluoride in the microbubbles, equivalent to 45 micrograms (**Figure 3**).

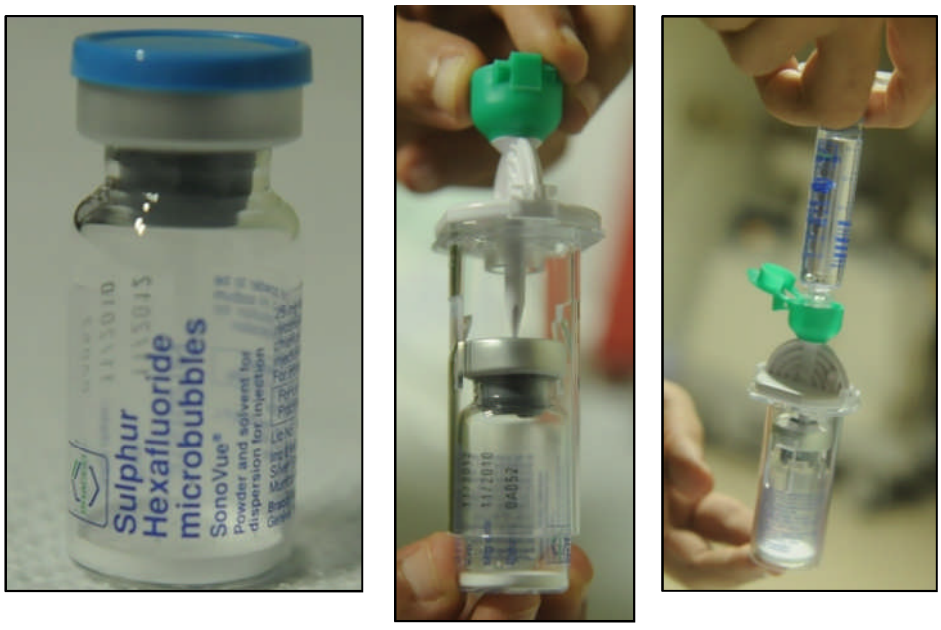

Figure 3: Ultrasound contrast medium SonoVue, Bracco

Contrast ultrasound investigations were performed after a short (1.5 ml) bolus injection into an antecubital vein (20-gauge Venflon) of Sonovue (Bracco Altana Pharma, Konstanz, Germany), being promptly followed by a 5 ml saline flush. The 15 MHz linear array probe, with a mechanical index varying from 0.4 to 1.4, with CPS continuous real-time recording software, was used to achieve the best visualization of the plaque morphology and vascularization. The 'contrast agent only' software feature, in which the image is derived only from the signals of the microbubbles, has been used. All the investigations were digitally stored and transferred to an external hard disk for the off-line analysis. After the study, the patients were monitored for 30 minutes to look for any adverse events.

CT angiography

MDCTA was performed using a 256 slice iCT scanner. Frontal and lateral topograms were obtained to define the correct filed-of-view (FOV). Axial sections of the brain were obtained parallel to the orbito-meatal line. Non-ionic iodinated contrast iohexol (Omnipaque, GE Healthcare, Shangai, China) was injected through an 18 gauge antecubital venous access (Venflon). 50 ml of 350mg/ml contrast was injected at a rate of 5ml/sec followed by 40ml of normal saline bolus chaser at the same rate. A real-time bolus tracking technique was used to synchronize the acquisition with passage of contrast. Threshold was set at 150 HU above baseline attenuation in the ascending aorta. Data acquisition was started after a post-threshold delay of 4.5 seconds. MDCTA acquisition parameters were as given in Table 1

Parameter	
Section thickness (mm)	0.9

Increment (mm)	0.45
Pitch	0.993
Rotation time (seconds)	0.5
kV	120
mAs/ slice	400
Collimation	128 x 0.625
Field of view (mm)	220
Matrix	512

MRI plaque imaging

MRI was performed on a 1.5Tclinical MR scanner (Magnatom Avanto; Siemens, Erlangen, Germany).

Patient preparation - MRI plaque imaging was performed as a separate study to maximize patient co-operation (not performed as a part of a brain or MR angiogram study). Prior to the MRI study, the carotid bifurcation on the affected was marked using B-mode ultrasound. The patients were counseled regarding the importance of lying still and avoiding swallowing. Appropriate positioning was performed with a head holder and coils were positioned at the level of carotid bifurcation marking.

Dedicated phased – array surface coils (carotid coils, Machnet, Eelde, the Netherlands; *http://www.machnet.nl/*) were used to increase the signal-to-noise ratio. Oblique scout view (3D PC, 2D TOF, 1 minute) was obtained. The carotid bifurcation was used as an

internal landmark to reproducibly prescribe slice locations for serial studies. Acquisition time was about 14 minutes.

Parameters used for the various sequences are given in Table2.

Sequence	**fse PD FS db**	**fse T2 FS db**	**fse T1 FS db**	**3D TOF**
Slices	16	16	16	48 in 1 slab
Slice thickness	2.9 mm	2.9 mm	3 mm	1 mm
Distance factor	0	0	0	-20.83
Phase encoding	A >> P	A >> P	A >> P	R >> L
Ph oversampling	80	60	70	60
FOV read mm	80	80	80	114
FOV phase %	100	100	100	75
TR msec	2750	2870	1110	29
TE msec	12	60	8.7	7.27
Flip angle degree	120	180	180	25
Resolution	192 x 100	192 x 100	192 x 100	320 x 75
Time mins	4.3	5.27	4.31	3.59

Image analysis

Ultrasound classification of plaques

Based on the B mode echogenicity, plaques were characterized as hypoechogenic, hyperechoic and hyperechoic with shadowing.

CEUS studies primarily focused on three areas of clinical importance:

1. enhancement of the carotid lumen and plaque morphology
2. identification of atherosclerotic-related neovascular changes within the adventitial vasa vasorum and plaques
3. identification of ulcerations/ irregularities on the surface of the plaque

UCA microbubbles seen moving with the plaque on dynamic scan were considered to indicate neovascularization.

CT angiography

Window level and window center were generally set at 700 HU and 200 HU respectively for optimum visualization of the vascular structures. After evaluating the axial source images, several reformatting techniques were utilized for assessing the carotid arteries: maximum intensity projection (MIP), multiplanar reconstruction (MPR), curved planar reconstruction (CPR) and volume rendering (VR). The degree of stenosis, location of plaque, surface irregularity/ulceration, calcification and attenuation of the plaque were studied.

Measurements to quantify the degree of stenosis were made by selection of a plane perpendicular to the lumen centerline using the NASCET criteria.

Plaque surface morphology was classified as smooth, irregular, or ulcerated. Plaque ulceration was considered as an outpouching of contrast material adjacent to or within the carotid wall, larger than 1 mm in width, exposing the necrotic core of the atheromatous plaque as described by Sitzer et al[83]. Ulcerated plaques were categorized according to the shape of the ulcer as Type 1 to 4 as previously described by Lovett et al[22].

The plaque density was calculated by drawing elliptical regions –of- interest in the predominant area of the plaque. Based on the density, carotid plaques were classified into three different groups[84]: fatty (soft) plaques defined as a plaque with a density value <50 HU; mixed (intermediate) plaque defined as a plaque with a density value between 50 and 119 HU; and calcified plaque defined as a plaque with a density value >120 HU. For each patient, the average value of three sample measurements in three contiguous axial was calculated for categorizing the patient.

MRI plaque imaging

We visually evaluated the signal of the carotid plaque and defined the main plaque component as the plaque feature that had the largest area among plaque range. The signal intensity of the main plaque component was compared to the signal intensity of the ipsilateral sternocleidomastoid muscle for each image sequence.

The various components of the plaques were classified as follows[55] (Table 3)

Plaque component	**T1**	**PD**	**T2**	**TOF**
Lipid-rich necrotic core	High	High	Variable (loss of signal as compared with PD)	Moderate
Fibrous tissue	Moderate	High	Variable (no loss of signal as compared with PD)	Moderate to low
Recent hemorrhage	High to moderate	Variable	Variable	High
Calcification	Low	Low	Low	Low

The scheme for evaluating MRI images is given in **Figure 4**.

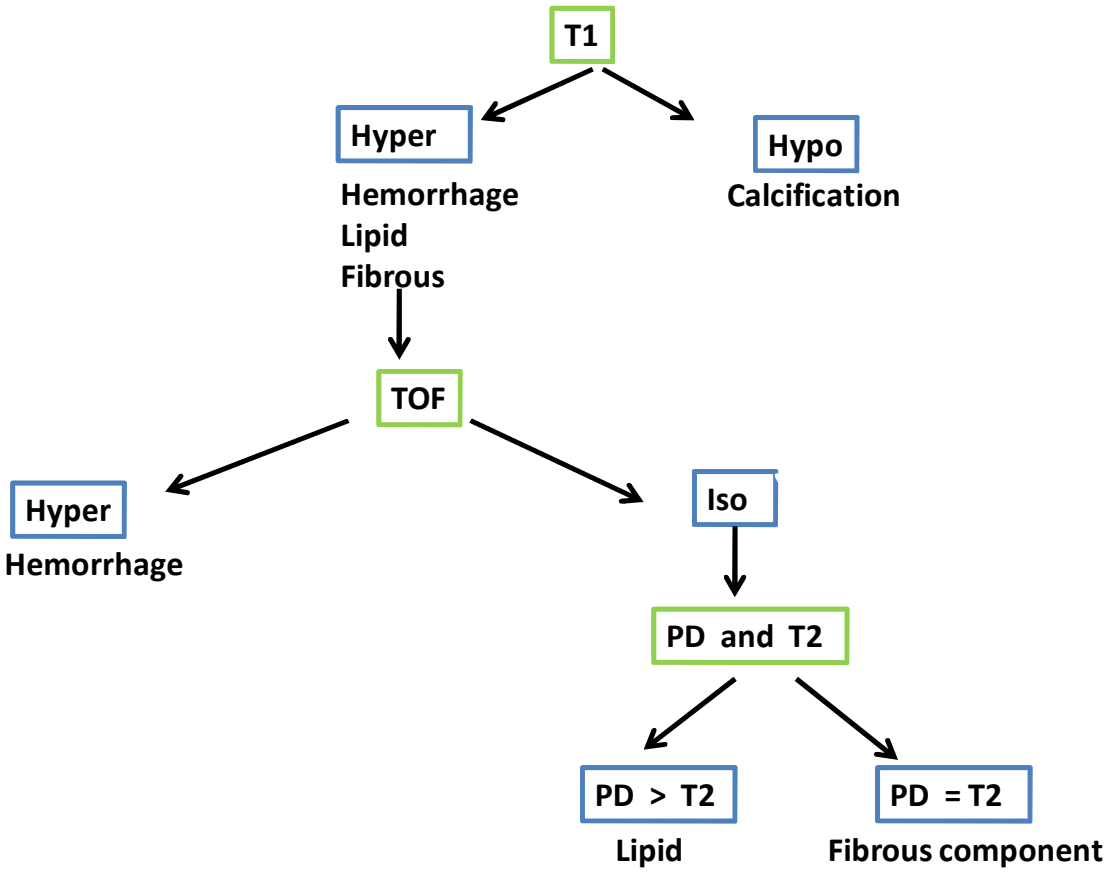

Figure 4: Flow chart for evaluating MRI

Statistical analysis

Statistical analysis was performed using Stata IC/11.2, StataCorps, College Station, Texas. Descriptive variables were described as mean and standard deviation. Plaques were dichotomized based on the presence or absence of neovascularization on CEUS and presence or absence of surface ulceration on CEUS, CTA and MRI. Agreements and kappa correlation coefficients between the various modalities were calculated. z test was used to calculate statistical significance. Two-sample t test with unequal variances was used to calculate the difference between mean CTA attenuation in various groups. A p value of <0.05 was considered to be statistically significant.

Results

26 patients were recruited. Examinations of two patients were excluded because of poor quality. Thus, we studied 26 carotid bifurcation plaques in 24 patients. Two patients (Sr no 18 and 24) had bilateral bifurcation plaque studies done. The mean age of patients was 65.41 ± 10.43 years with an age range of 45 to 80 years. 21 (87.5%) of our patients were males, three were females.

Four plaques caused moderate carotid stenosis (50-70%) and 23 had severe stenosis (70-99%). The mean stenosis (± SD) by NASCET criteria was 75.85 ± 14.7 with a range of 50 – 99%.

Baseline characteristics of the study population are given in Table 4.

Age, years; mean ±SD	65.13 ± 10.56
Symptomatic artery	
Right	8
Left	13
Bilateral	1
Asymptomatic patients	2
Bilateral plaques	9
Cerebrovascular symptoms	
TIA	15
Number of TIAs (mean, median)	1-more than 10 (3.3; 1)
Stroke	14
Risk factors	

Smoking	2 current; 5 reformed
Hypertension	15
Diabetes	14
Hypercholesterolemia	3
Cardiac disease (coronary artery disease)	6

B mode ultrasound (grey scale) evaluation

All 26 plaques in 24 patients were evaluated with B mode ultrasound. The echogenicity of the plaques was studied. Of 26 plaques, 12 (46.15%) were hypoechoic, 10 were hyperechoic and four were hyperechoic with shadowing. 14 (53.85%) plaques had hyperechoic components. Surface ulceration was seen in two of the 24 plaques.

Contrast – enhanced ultrasound

Contrast – enhanced ultrasound was performed in 18 plaques (16 patients). When using a reduced mechanical index for imaging, the plaques and corresponding intima–media complex appeared hypoechoic, whereas the adventitial layer was observed as echogenic. Ultrasound contrast agent (UCA) microbubbles were visualized few seconds after the bolus injection as a hyperechoic dynamic flow in the carotid vessel lumen, providing an enhanced visualization of the carotid intima-media complex and a better identification of the plaque surface and the degree of stenosis.

Few seconds after the contrast agent detection in the carotid lumen, the dynamic distribution of the UCA inside the plaque allowed the visualization of the plaque vascularization.

Plaque neovascularization was seen in ten of the 18 plaques studied (55.56%). Only 1 of these 10 plaques was asymptomatic, while 2 of the remaining 8 patients were asymptomatic

Vascularization was detected at the shoulder of the plaque on the adventitial layers, and in the iso-hyperechoic fibrous and fibro-fatty tissue. It was represented by little echogenic spots rapidly moving within the texture of the atheromatous lesion, easily identifiable in the real-time motion, and depicting the small microvessels. The diffusion of the contrast agent appeared to be in an 'outside-in' direction.

Ulceration of the surface was detected in four out of 18 plaques (22.22%). Three out of four ulcerations were associated with neovascularization. All 4 ulcerated plaques were symptomatic.

The examination was well tolerated in all patients with no adverse events.

CT angiogram

CTA was performed in 18 patients. 19 (73.08%) plaques were studied. The attenuation of plaques (excluding the calcified components ranged from 4.8 to 79 HU with a mean of 49.82 $\pm$ 19.66 HU. 15 out of 19 (78.95%) plaques had calcification. Surface ulceration was seen in eight out of 19 (42.11%) plaques. One of the 19 plaques had two ulcerations, of which one was type 3. One more plaque had a type 3 ulcer. All the remaining ulcers were type 1.

Plaque Surface Morphology Characteristics of 19 Atherosclerotic Carotid Arteries on CTA (Table 5)

Carotid arteries with atherosclerosis	Number (%)
Smooth surface	10
Irregular surface	2
Ulcerated surface	7
No. of ulcerations per carotid artery	
1	6
>1	1
Type of ulceration	
1	6
2	0
3	2
4	0

MRI plaque imaging

19 patients underwent MRI plaque imaging of 20 (76.92%) carotid bifurcations. Based on the predominant components of the plaque, plaques were characterized as lipid (3), lipid with recent hemorrhage (1), fibrous (7), fibrofatty (4), fibrofatty with some hemorrhagic components (3) and recent hemorrhage (2).

An intact fibrous cap was visualized in 9 patients. Surface ulceration was visualized in 10 patients. In one patient, the fibrous cap was not visualized. The surface ulceration also could not be seen.

The signal intensity on various pulse sequences and surface characteristics are as described in Table 6.

Sr no	PD	T2	T1	TOF	Composition	Fibrous cap	Ulcer
1	iso	hypo	mildly hyper	iso	lipid	y	n
2	iso	hypo	hyper	hyper	lipid with recent he	n	y
3	iso	iso	mildly hyper	iso	fibrous	y	n
4	hyper	hyper	hyper	iso	blood thrombus	n	n
5	iso	iso	mildly hyper	iso	fibrous	y	n
6	iso	hypo with small hyper component	small hyper comp	iso	fibro-fatty with small he	n	y
7	iso	iso	mildly hyper	iso	fibrous	n	n
8	iso	hypo	mildly hyper	iso	lipid	n	n
9	iso	iso	mildly hyper	iso	fibrous	n	y
11	hyper	hyper	mildly hyper	hyper	hemorrhagic	n	y
14	iso	iso	mildly hyper	iso	fibrous with little lipid	y	y
15	iso	hypo	mildly hyper	iso	fibro-fatty	y	y
17	hyper	hyper	hyper	hyper	hemorrhagic	n	y
18	iso	iso,	iso	iso	fibrous	y	n
18	iso	hyper	hyper	hyper	fibrofatty with he	y	n
19	iso	iso	mildly hyper	iso	fibrous	y	n
20	iso	iso	mildly hyper	iso	fibrofatty	y	y
21	iso	hypo	mildly hyper	iso	lipid	y	y
22	iso	hypo with small hyper component	small hyper comp	iso	fibro-fatty with small he	n	y
23	iso	hypo	iso	iso	fibrofatty	y	n

Comparison of plaque composition by MRI and ultrasound B mode echogenicity

20 plaques in 19 patients had undergone both MRI and B mode ultrasound evaluation. Observed agreement between these tests was 75% and expected agreement was 59% with a kappa value of 0.39 (fair agreement) with a significant p value (p= 0.03).

Crosstable of MRI and plain US echogenicity (Table 7)

	Plain US		
MRI	Hypoechogenic	Hyperechogenic	Total
Lipid	3	1	4
Others	4	12	16
Total	7	13	20

P = 0.03*

Key – 'Other' in MRI plaque include fibrous, fibrofatty without or with hemorrhage or hemorrhagic; Hyperechogenic in plain US includes without and with shadowing

Comparison of B mode ultrasound and CEUS

Of the18 plaques evaluated with CEUS, neovascularization was seen in 10. Of these, 7 were hyperechoic and 3 were hypoechoic. Of the 8 plaques without neovascularization, 4 were hypoechoic.

Comparison of MRI and CEUS

11 patients underwent both MRI and CEUS of 12 plaques. 5 plaques did not show any enhancement. Of the 7 plaques that did show enhancement, 2 were fibrous, 1 was fibrofatty, 2 were fibrofatty with some hemorrhage and 2 were hemorrhagic. None of the plaques with predominantly lipid content shows neovascularization.

Ulceration was seen both on MRI and CEUS in 2 plaques, only on CEUS but not on MRI in 2 plaques and only on MRI but not on CEUS in 4 plaques. Ulceration was seen neither on CEUS or MRI in 4 plaques.

Comparison of plaque composition by CTA attenuation and ultrasound B mode echogenicity

19 plaques were evaluated by both CTA and B mode ultrasound. There was 52.63% observed agreement and 49.86% expected agreement between the tests with a kappa value of 0.05 (slight) with p=0.4 (not significant).

Crosstable of plain US echogenicity and CT attenuation (<50 vs 50- 119 HU) (Table 8)

	CT		
Plain US	<50HU	50-119 HU	Total
Hypoechogenic	5	5	10
Hyperechogenic	4	5	9
Total	9	10	19

Attenuation of plaques according to echogenicity (Table 9) (Figure 5)

Group	**Number of plaques**	**Mean**	**Std deviation**	**95% confidence interval**	
Hypoechogenic	10	47.66	22.88	31.39	64.03
Hyperechogenic	9	52.22	16.38	39.63	64.82
Combined	19	49.82	19.66	40.34	59.3
Difference		-27			

Two-sample t test with unequal variances, p = 0.62

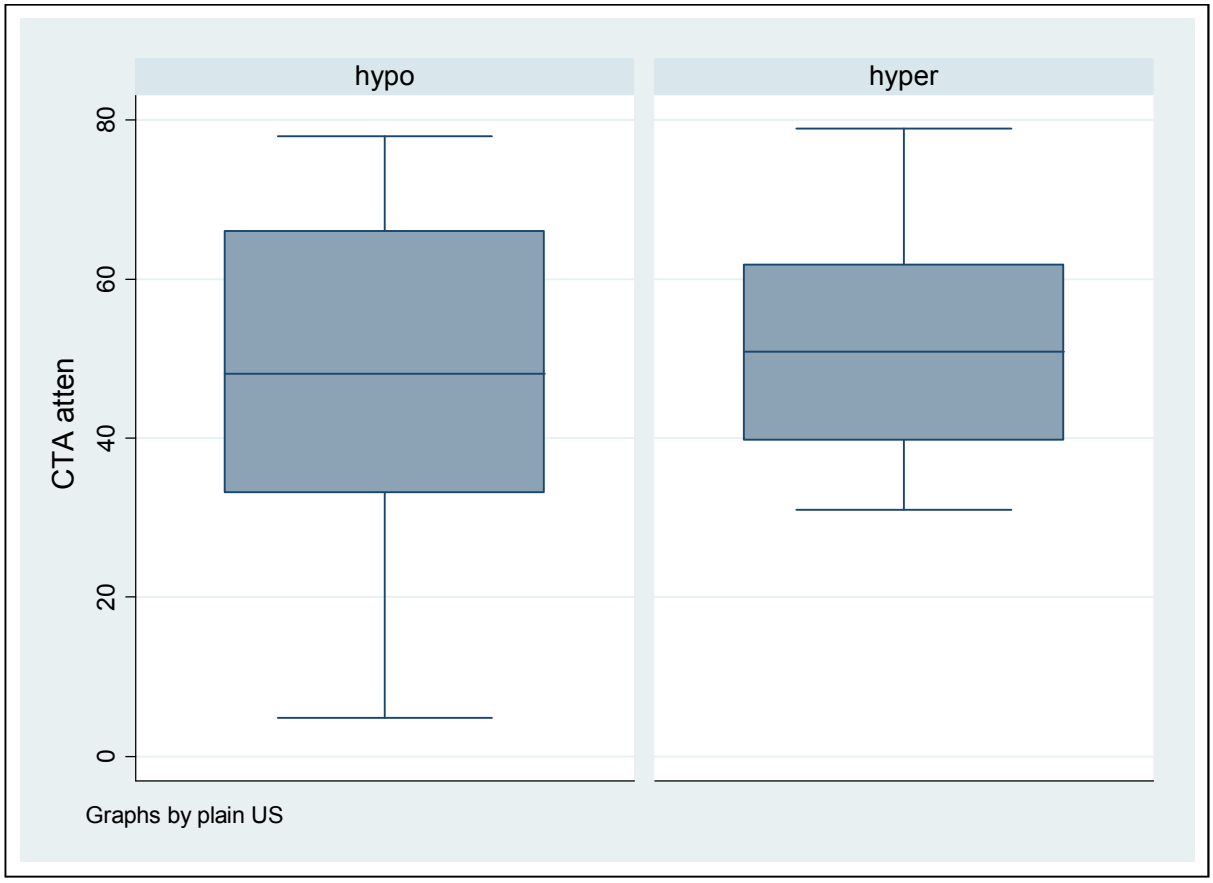

Figure 5: Box and whisker plot of CTA attenuation of hypoechoic and hyperechoic plaques on B mode ultrasound

Comparison of MRI and CTA

13 patients (14 plaques) had both MRI and CTA imaging available.

Of these, 3 patients had predominantly lipid or fibrofatty core with a density range of 28.9 to 66.1 HU and a mean density of 44.53 HU.

Three patients had a predominantly fibrous core with a density range of 56.9 to 73.3 HU and a mean density of 64 HU.

One patient had a predominantly hemorrhagic core with a density of 52.9 HU. One patient had an intraluminal thrombus with a density of 50.9 HU.

The observed agreement between MRI composition and CT attenuation (<50 vs 50- 119 HU) was 78.57% and expected agreement was 54.08% with a kappa value of 0.53 (moderate correlation), p= 0.01

Crosstable of MRI and CT attenuation (<50 vs 50- 119 HU) (Table 10)

	CT		
MRI	<50HU	50 – 119 HU	Total
Lipid	3	0	3
Others	3	8	11
Total	6	8	14

p = 0.01*

The mean attenuation of plaque with predominantly lipid content was 38 HU and other plaques (fibrous / fibrofatty / hemorrhagic) was 58HU, p value was statistically significant (p = 0.0001) (Table 11)

Group	Number of plaques	Mean	Std deviation	95% confidence interval	
Lipid	3	31	2.1	25.78	36.22
Others	11	58	15.04	47.89	68.12
Combined	14	52.21	17.52	42.1	62.33
Difference		-27			

Two-sample t test with unequal variances, p = 0.0001*

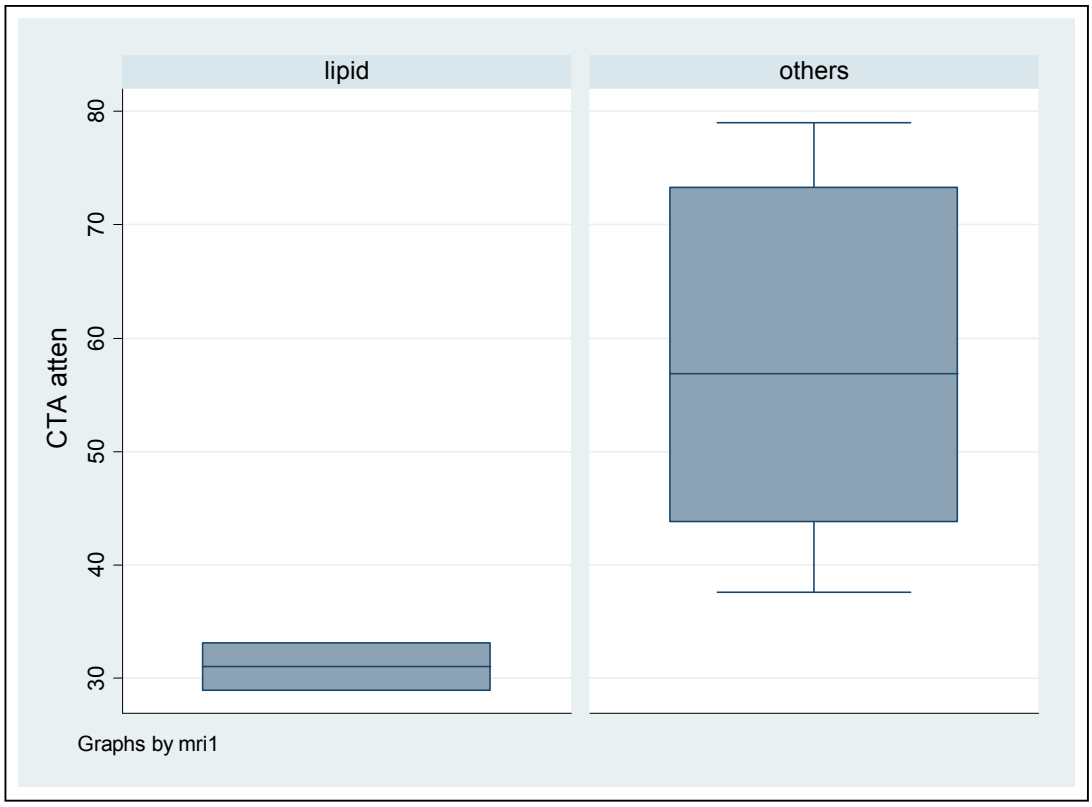

Figure 6: Box and whisker plot of CTA attenuation of plaques by composition on MRI.

Comparison of CEUS and CTA

11 patients (13 plaques) had both CEUS and CTA imaging available.

Of these, 8 plaques had neovascularization seen on CEUS. The average attenuation of these plaques was 52.14 $\pm$ 16.74 HU (range 37.6 to 56.9 HU). Of the 5 plaques without neovascularization on CEUS, the average attenuation was 40.26 $\pm$ 22.87 HU (range 4.8 to 74 HU), p = 0.35 (Figure 7)

Table 12 – Cross table of neovascularization seen on CEUS with CT attenuation (<50HU vs 50-119HU)

	CT attenuation		
CEUS	<50HU	50-119HU	Total
n	3	2	5
y	4	4	8
Total	7	6	13

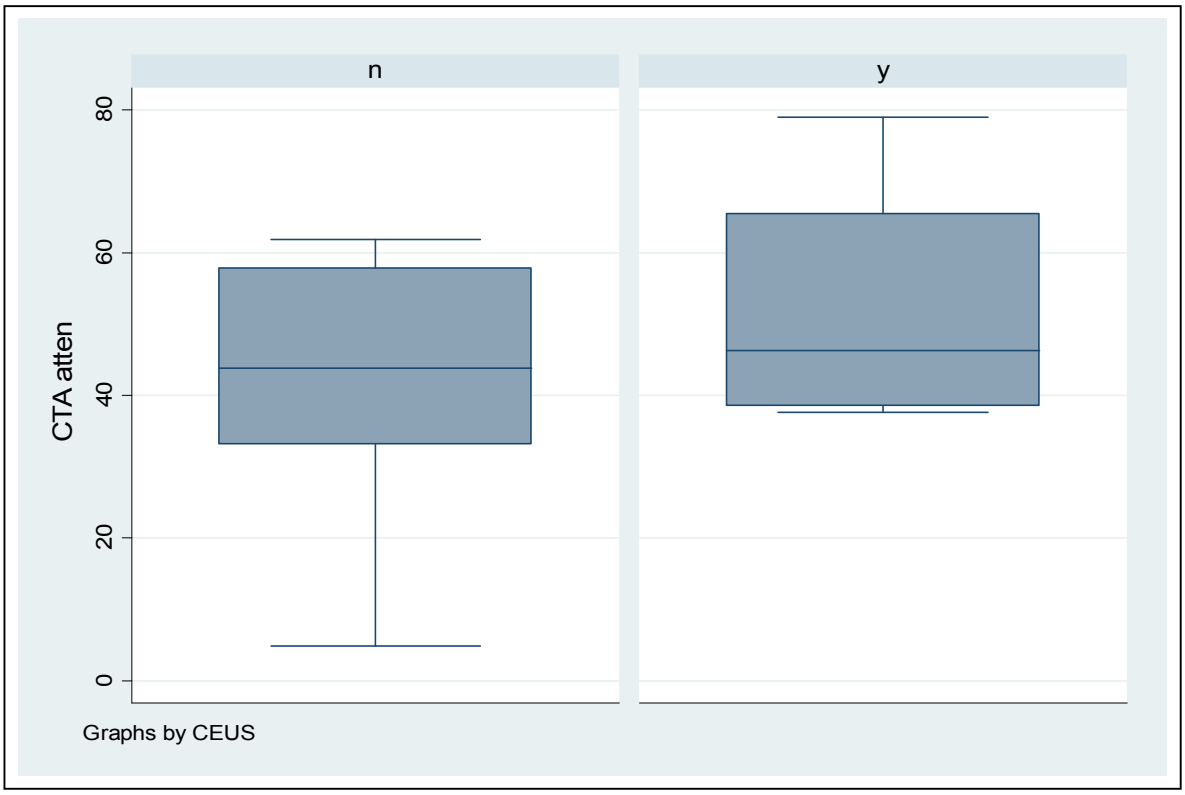

Figure 7: Box and whisker plot of CTA attenuation of plaques with (y) and without (n) neovascularization.

Table 13

Modality and ulceration	CEUS		
MRI	Absent	Present	Total
Absent	3	0	3
Present	6	3	9
Total	9	3	12

The observed agreement between detection of ulceration by MRI and CEUS was 50% and expected agreement was 37.5% with a kappa value of 0.2 (slight agreement), p= 0.12.

Table 14

Modality and ulceration	CTA		
MRI	Absent	Present	Total
Absent	5	0	5
Present	1	8	9
Total	6	8	14

The observed agreement between detection of ulceration by MRI and CTA was 92.86% and expected agreement was 52.04% with a kappa value of 0.85 (almost perfect agreement), p= 0.0006.

Table 15

Modality and ulceration	CTA		
CEUS	Absent	Present	Total
Absent	6	4	10
Present	1	2	3
Total	7	6	13

The observed agreement between detection of ulceration by CEUS and CTA was 61.54% and expected agreement was 52.07% with a kappa value of 0.2 (slight agreement) p= 0.20.

Representative cases

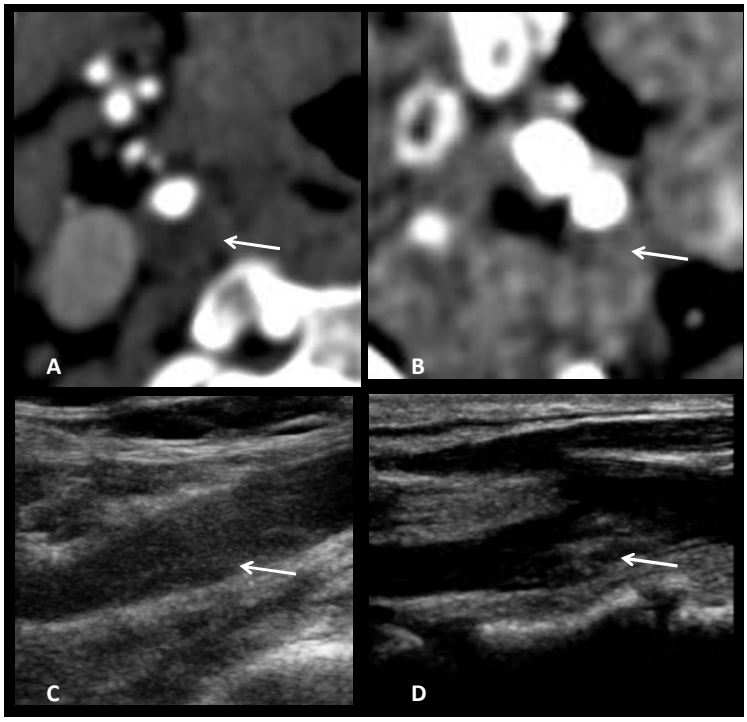

Figure 8: Attenuation of plaques as seen on CTA (A) 4.8 HU; (B) 66.1 HU; On B mode ultrasound (C) hypoechoic and (D) hyperechoic plaque

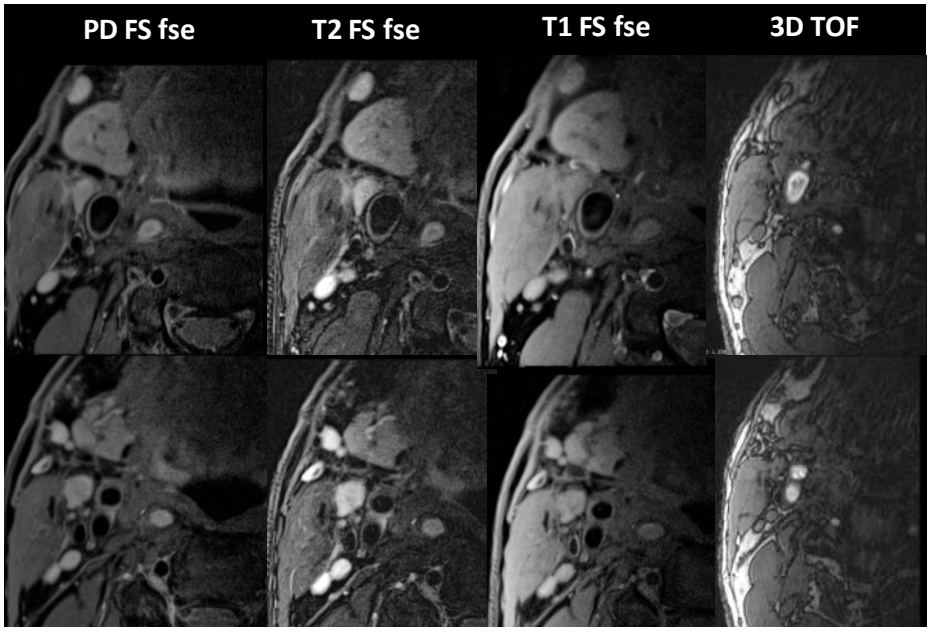

Figure 9: MRI plaque imaging performed on a normal volunteer.

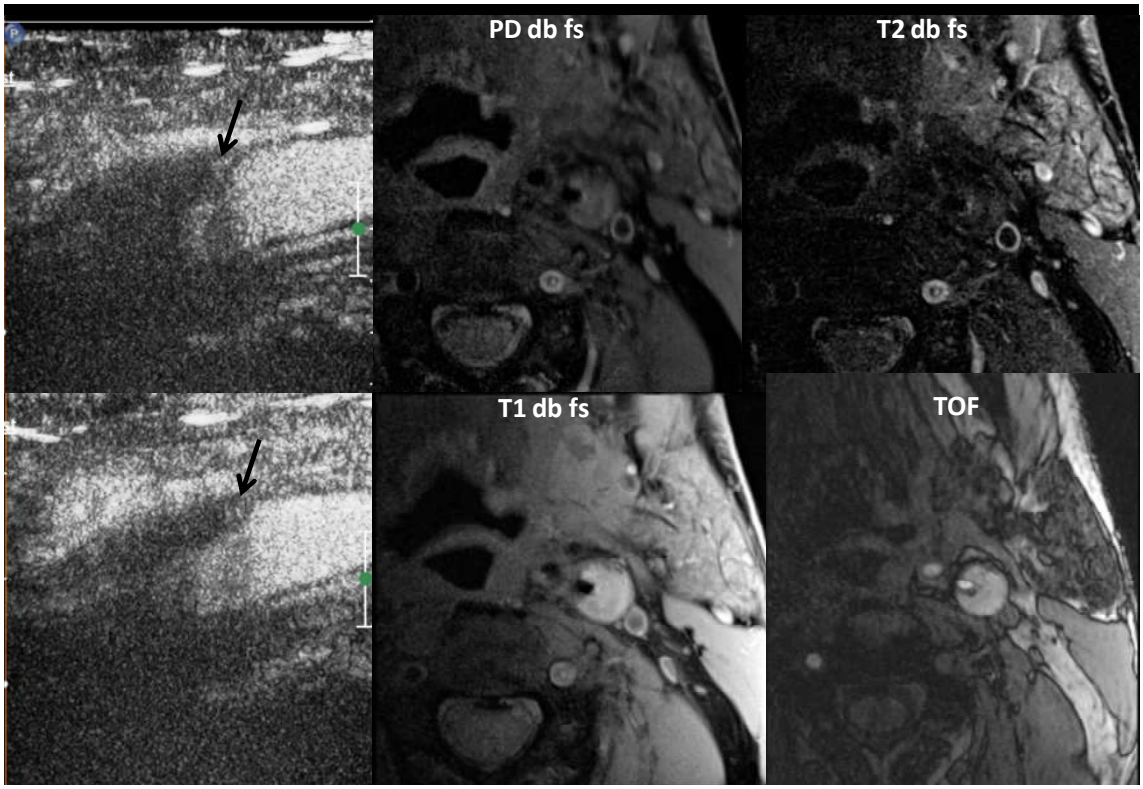

Figure 10: M/ 71 yrs with left MCA stroke. Left ICA 80% stenosis. On CEUS, moving microbubbles are seen on the shoulder of the plaque (black arrows). On MRI plaque imaging, it appears isointense on PD, hypointense on T2WI a with small hyperintense component and hyperintense on T1WI and TOF s/o fibro-fatty plaque with a small hemorrhagic component. Surface ulceration is present.

Figure 11:(next page 51)M/67 yrs with left MCA and MCA- ACA watershed territory stroke. On CTA, left ICA 80% stenosis. Plaque has attenuation of 37.6 HU. A type III ulceration is present (dotted white arrows). On CEUS, plaque neovascularization is seen with surface irregularity. On MRI plaque imaging, plaque appears isointense on PD and hypointense to isointense on T2WI. It is mildly hyperintense on T1WI and isointense on TOF images s/o fibro-fatty plaque. Surface ulceration is present. On MRI, plaque appears isointense on PD, hypointense on T2WI, mildly hyperintense on T1WI and isointense on TOF s/o fibro-fatty plaque. Fibrous cap is seen but it is discontinuous at places s/o surface ulceration.

Figure 11 (legend on previous page)

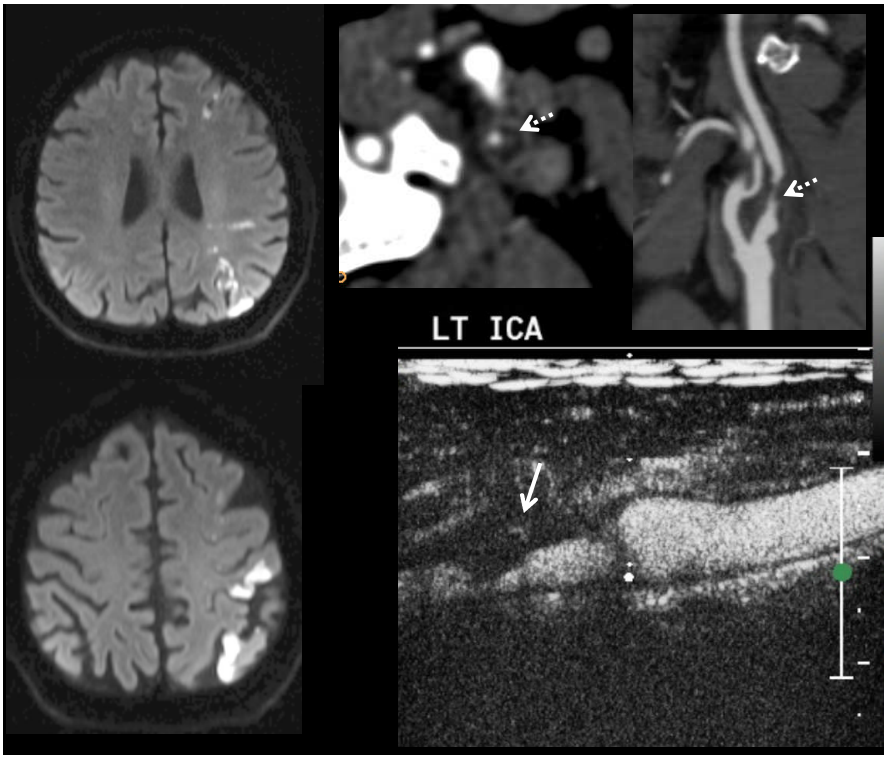

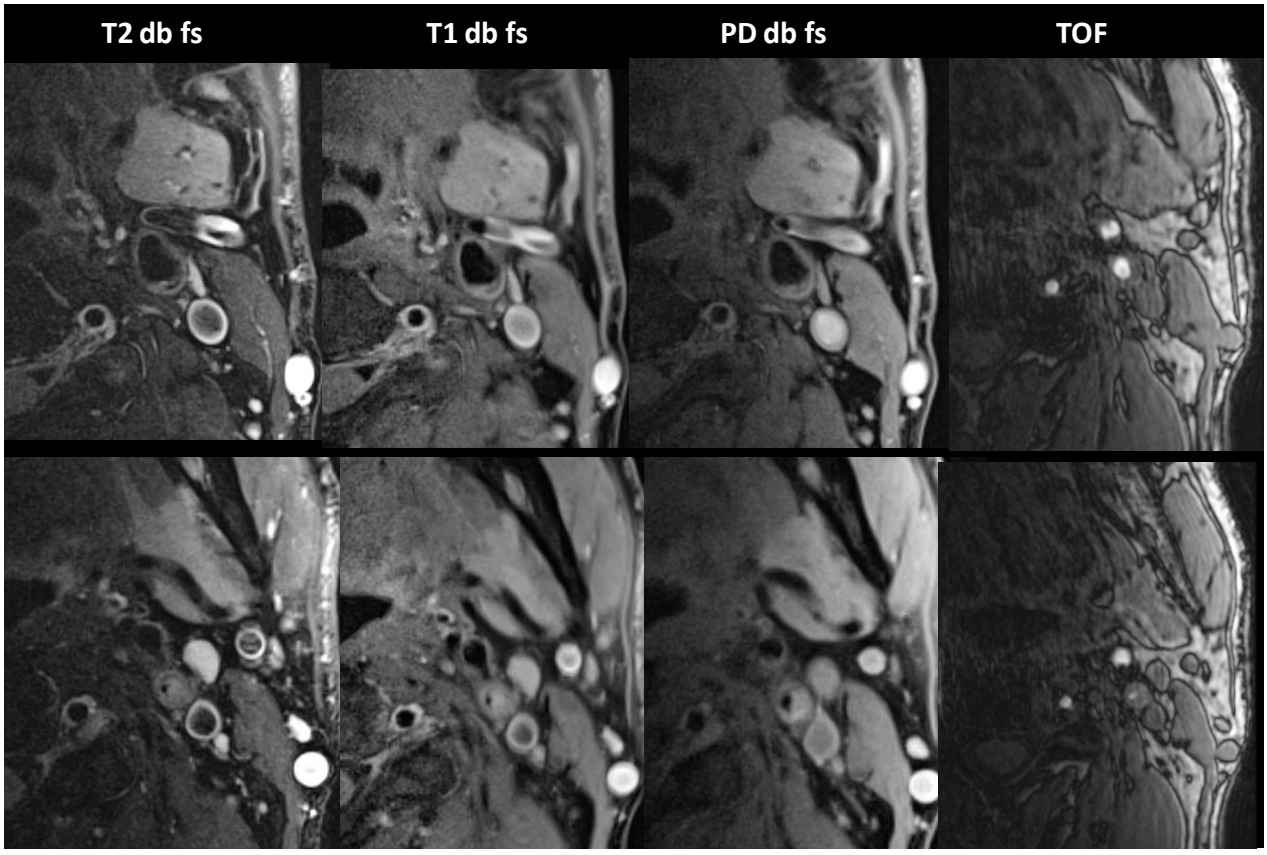

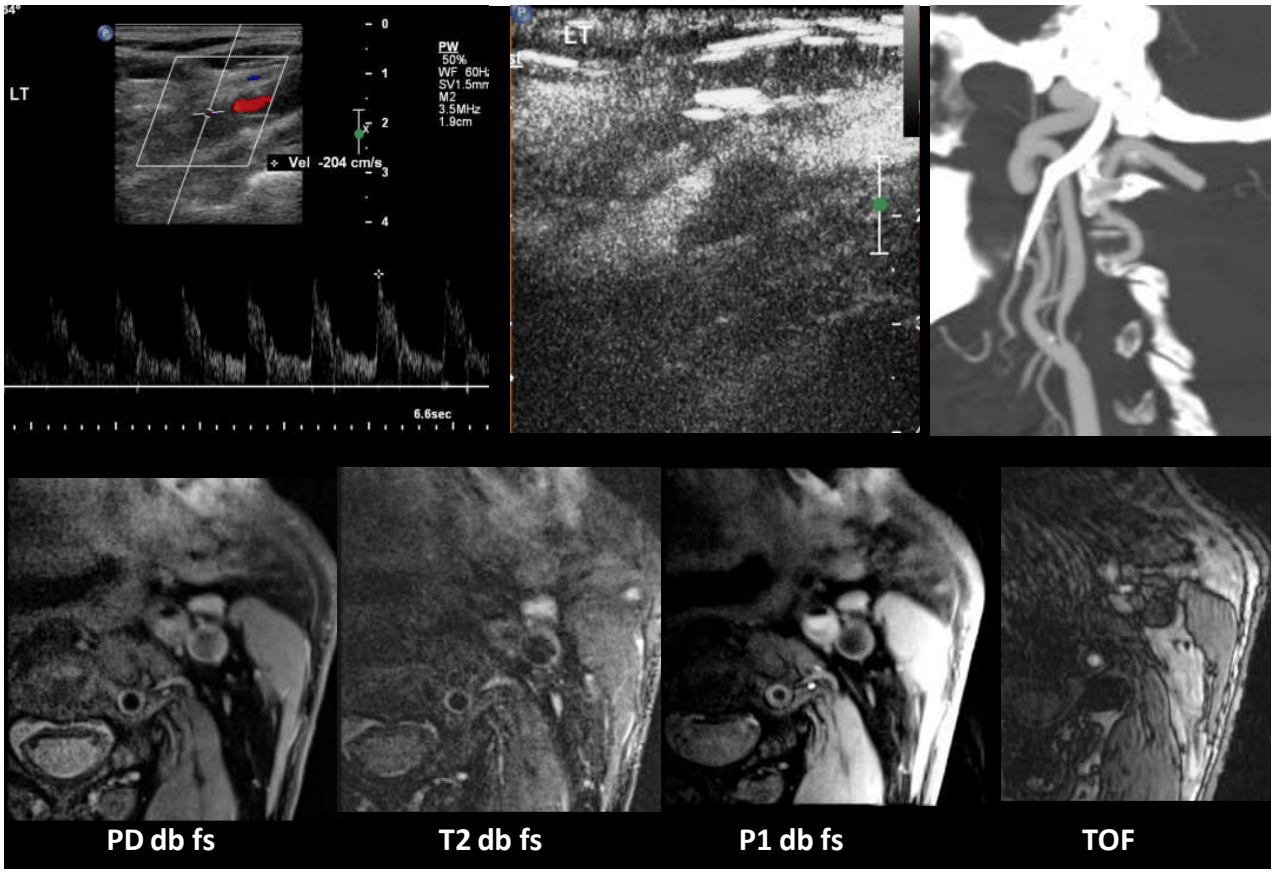

Figure 12: M/ 80 yrs with4 episodes of left MCA TIAs. Left ICA 80% stenosis. PSV 204 cm/s No neovascularization is seen on CEUS. On CTA, plaque is hypoattenuating and surface shows a single Type III ulceration. On MRI, plaque appeared isointense on PD, hypointense on T2WI, mildly hyperintense on T1WI and isointense on TOF s/o lipid core. Fibrous cap was well visualized.

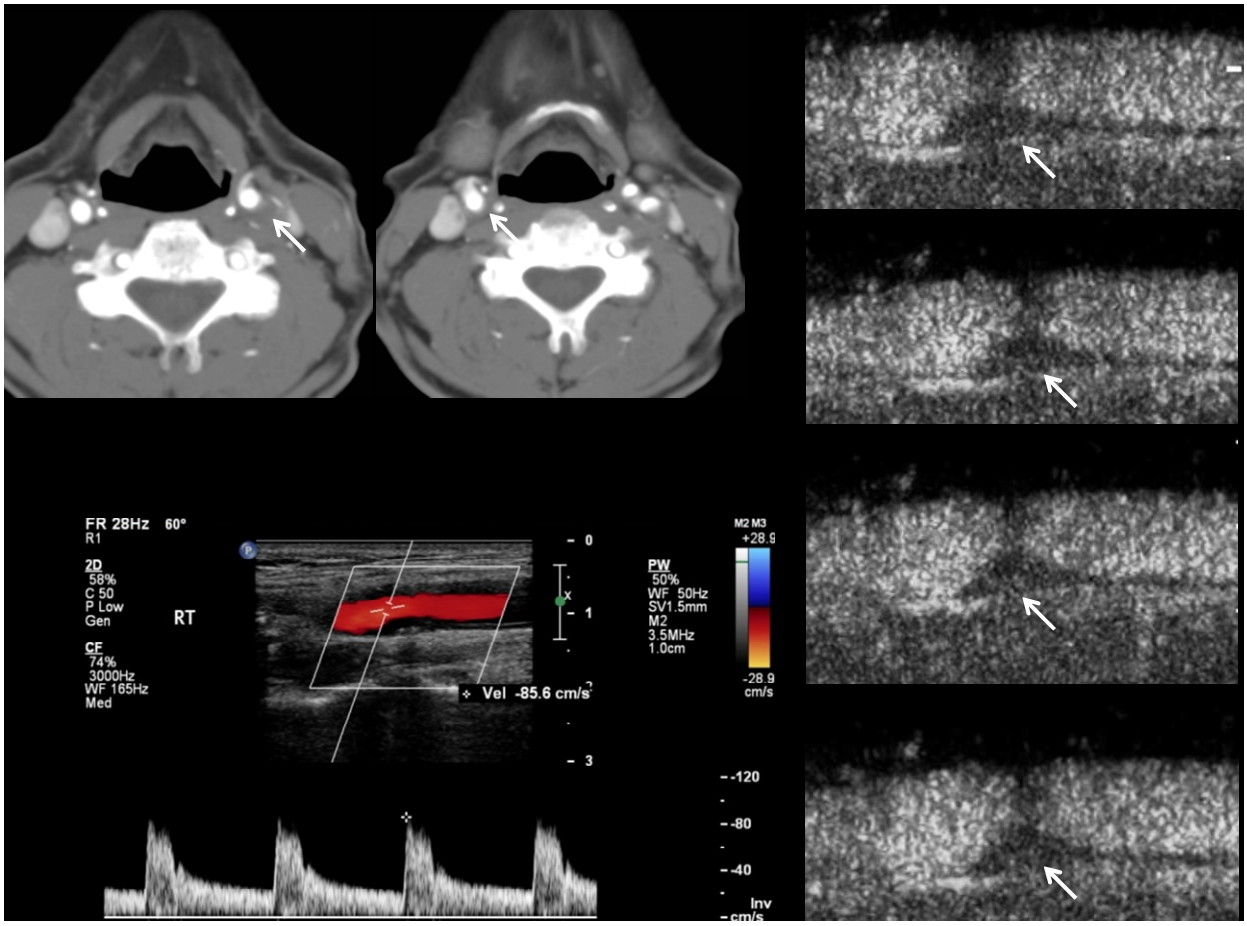

Figure 13: M/ 72 yrs with left hemiparesis. Right ICA 50% stenosis. PSV 85.6 cm/sec. CEUS shows moving microbubbles in the plaque (images at different time frames).

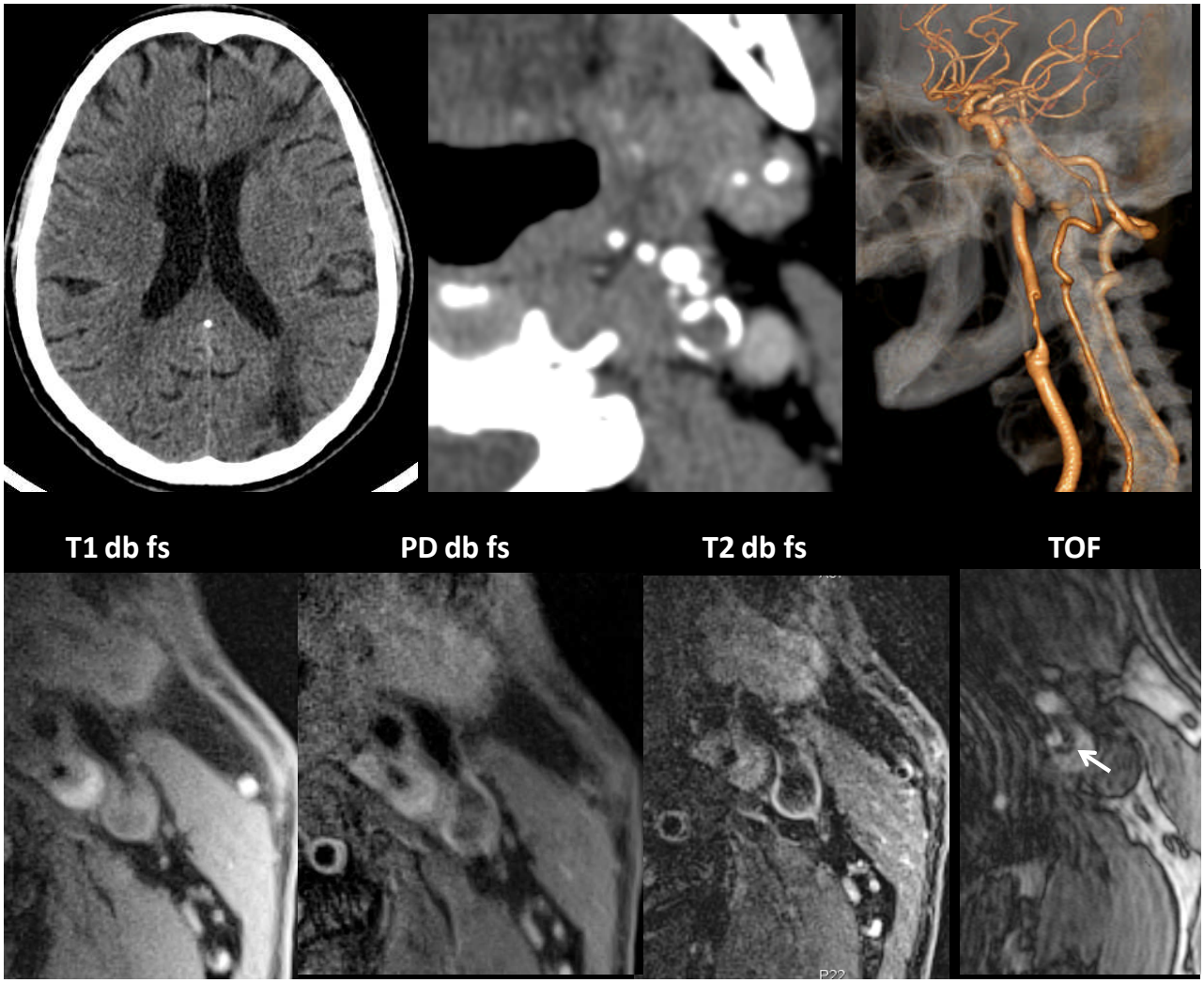

Figure 14: M 75 yrs with left carotid plaque. It is hyperintense on all pulse sequences suggestive of recent hemorrhage. Surface ulceration is present (arrow in TOF)

Discussion

Atherosclerosis causing carotid artery stenosis is an important preventable and modifiable cause of ischemic stroke, accounting for about 25% of the cases[85] and also for the majority of myocardial infarctions and sudden cardiac deaths. The natural histories of equally severe symptomatic and asymptomatic carotid stenoses are different, suggesting a dichotomy in plaque behavior.[5]

Large randomized trials such as the NASCET[86] or the European Carotid Surgery Trial[87] have shown the benefit of CEA for recently symptomatic patients with severe (>70%) stenosis. The optimal treatment strategy in symptomatic patients with mild/moderate (30%–70%) carotid stenosis or in asymptomatic patients, however, remains unclear. For example, additional evaluation of the NASCET data found that of the 2226 symptomatic subjects with <70% stenosis, 61% had < 50% stenosis. The role of CEA in asymptomatic individuals is also still much debated in light of the results of the Asymptomatic Carotid Atherosclerosis Study[88] and the Asymptomatic Carotid Surgery Trial.[89] Various interpretations of these 2 studies have lead to discrepant recommendations of optimal treatment strategies.

Imaging methods have the potential to be used as a screening tool for the presence of atherosclerosis and the degree of stenosis. Imaging also helps to distinguish stable from vulnerable plaques and ultimately to distinguish patients with low versus those with high risk of cardiovascular complications. “Vulnerable” plaques are atherosclerotic plaques that have a high likelihood to cause thrombotic complications, such as myocardial infarction or stroke. Plaques that tend to progress rapidly are also considered

to be vulnerable.[90] The concept of ‘‘vulnerable plaque’’ was first introduced for coronary arteries[2] and later expanded to the carotid circulation.

Glagov et al[91] first described the phenomenon of vessel remodeling, which means that large plaques can develop through outward expansion of the vessel with little resultant luminal stenosis. Thus, the degree of stenosis may not accurately measure the plaque burden.

The degree of stenosis has been associated with symptoms in various studies. This was traditionally measured on carotid angiography. However, carotid angiography does not demonstrate plaque morphology, with the exception of luminal ulceration, and the degree of stenosis is not associated with the presence of intraplaque hemorrhage or a necrotic core.[2] Thus, the degree of stenosis may not necessarily predict the vulnerability. Besides luminal stenosis, plaque composition and morphology are key determinants of the likelihood that a plaque will cause cardiovascular events. The challenge for screening and diagnostic imaging methods is to identify patients at high risk who have lesions that are vulnerable to thrombosis, so-called vulnerable plaques, before the event occurs.

Pathology of carotid atherosclerosis

Atherosclerosis commonly occurs near branch ostia, bifurcations, and bends, suggesting that flow dynamics play an important role in its induction.[92] Atherosclerotic plaque tends to occur at regions where flow velocity and shear stress are reduced.[93] It has been demonstrated that blood flow is disturbed at the carotid bifurcation, where it departs from a laminar unidirectional pattern. The greatest atherosclerotic plaque accumulation typically occurs on the outer wall of the proximal segment and the sinus of the internal

carotid artery, in the region of the lowest wall shear stress. Plaque is thinner on the flow divider side at the carina of the internal and external carotid arteries, where wall stress is the highest.

Thus, the flow properties of the carotid bifurcation contribute to the initiation of atherosclerotic plaque. This plaque passes through various stages of evolution.[94,95]

The early lesions consist of two distinct nonatherosclerotic intimal lesions, intimal thickening and intimal xanthoma ("fatty streak"). The precursor lesion in most progressive lesions is pathologic intimal thickening which is a transition between early lesions of atherosclerosis and the more advanced fibroatheroma. The fibrous cap atheroma is the first advanced lesion of coronary atherosclerosis. It is composed of a lipid-rich necrotic core encapsulated by fibrous tissue. The origin and development of the necrotic core occurs by invasion of macrophages, and their apoptosis. The fibrous cap atheroma may result in significant luminal narrowing and is prone to complications of surface disruption, thrombosis, and calcification. Intraplaque hemorrhage arises from the disruption of the intraplaque thin-walled microvessels (vasa vasorum). Intraplaque hemorrhage and rupture of the fibrous cap are associated with an increased density of microvessels.

Mauriello et al[96] define vulnerable plaques in the carotid artery as plaques that have a thin fibrous cap less than 165 μm with associated macrophage infiltration, are CD68 positive, and number more than 25 per high-power field, without plaque rupture.

Plaque rupture with erosion/ ulceration is the dominant mechanism leading to thrombus formation with subsequent embolization and cerebral ischemic events.[97]

Infiltration of inflammatory cells to the surface of carotid plaques is a critical step in promoting plaque rupture and resultant embolization or carotid occlusion.[98]

Healed lesions, the third category of atherosclerotic disease, consist of healed plaque ruptures (HPRs), erosions, and eventual total occlusions.

Fibrocalcific plaques are characterized by thick fibrous plaques overlying extensive accumulation of calcium in the intima close to the media or lumen.

Plaque Vulnerability

The histologic hallmarks of vulnerable plaques include a larger lipid core (>40% of total lesion area), a thinner fibrous cap, many inflammatory cells,[99,100] calcified lesions[101] and neoangiogenesis.[102]

T lymphocytes may be central to plaque instability. T cells can induce macrophages to secrete MMPs via stimulation of CD40, and in addition, through production of interleukin-1, can promote smooth muscle cell apoptosis.[103] Because plaque rupture depends on a balance between the tensile strength of the plaque and stress exerted on it, rupture is likely triggered by a sudden increase in stress on the plaque or, less likely, by a sudden reduction in plaque strength. Possible causes include sudden increases in blood pressure or pulse rate (eg, during exercise or sympathetic system stimulation), vasospasm forcing plaque contents through a weakened plaque cap, and hemorrhage into the plaque.

Eliasziv et al[23] have shown that the presence of ulceration represents an important risk for neurologic symptoms.

Vasa vasorum are physiological structures that provide nourishment to the vessel wall and play an important role in the pathogenesis of atherosclerosis. They are normally present in the adventitia. The work of ***Koester***[104] in 1876 and ***Winternitz***[105] in 1938 first implicated them in the pathophysiology of atherosclerosis.

Techniques for imaging atherosclerotic plaques

Methods commonly used in imaging patients with atherosclerosis imaging include B-mode ultrasonography (US) and doppler, intravascular US, conventional angiography, computed tomography (CT), and magnetic resonance (MR) imaging. The digital subtraction angiogram (DSA) represents the traditional and gold standard method for assessing the severity of luminal narrowing in the carotid artery. Using DSA, the clinician can accurately observe and measure the luminal diameter along the length of the artery in a two-dimensional plane; moreover, he or she can visualize flow characteristics, such as separation and eddies.

The disadvantages of DSA include non-visualization of the wall and also its invasive nature. It is labour, time and material intensive. Only two dimensional images are provided.

Optimization of protocol

The first step in our study was to standardize the protocols for MRI plaque imaging and CEUS as these studies were not being routinely performed. With this aim, we initially performed MRI on healthy volunteers without carotid artery disease (n=9) for optimizing the sequences for image quality and time with the help of applications specialists. We later performed the same in asymptomatic patients (n=5) with carotid artery disease who were fit enough to cooperate for the scans. Similarly, we also

performed a few test scans of CEUS in asymptomatic patients (n=3) with carotid artery disease who were fit enough to cooperate for the scans. This initial optimization and learning curve phase was not included in our study analysis.

The carotid ultrasound examination

Doppler ultrasound provides an inexpensive, fast, noninvasive technique to assess carotid lesions. It can provide local diameter and wall thickness measurements as well as flow characteristics, including waveforms, gradient, and peak velocities. However, it is operator dependent.

Based on the European Carotid Surgery Trial (ECST)[87] and the North American Symptomatic Carotid Endarterectomy Trial (NASCET),[86] the degree of luminal stenosis and recent focal neurological symptoms are considered important for stroke risk stratification. This measurement of stenosis was initially performed on DSA. Extensive work has been undertaken in the generation of reliable and reproducible criteria for the calculation of internal carotid artery stenosis using unenhanced duplex ultrasonography. This is based on largely velocity criteria, is standardised and been used in the creation of national and international society consensus documents.[106-109] Duplex ultrasonography is likely to remain the first line imaging modality in this context. However, before performing carotid endarterectomy, a second imaging modality is used for confirming the percentage stenosis. The ACST trial[110] also identified a subgroup of asymptomatic patients who would benefit from carotid endarterectomy.

Apart from the degree of stenosis, B mode ultrasound can also give information regarding the plaque composition. We did not find other studies comparing plaque

compostion on B mode ultrasound with CTA and MRI. In our study, we found fair agreement between USG and MRI but only slight agreement between MRI and CTA.

Neurological symptoms are associated with a number of histological patterns, such as higher immature microvessel density, subsequent intraplaque haemorrhage and fibrous cap rupture.[18,19,111] Angiogenesis is also related to an increased inflammatory infiltrate and plaque instability.[112,113] Thus, plaque characterization and neovascularization could be an important adjunct for stroke risk stratification in patients with asymptomatic carotid artery stenosis. The mean attenuation of plaques with neovascularization was lower than that of plaques without neovascularization. When we compared the incidence of neovascularization of plaques echogenicity of plaques on B mode USG, 70% of our plaques were echogenic. Coli et al[38] had found that echoleucent plaques had higher degree of contrast enhancement.

Potential problems with contrast enhanced ultrasound

There is a theoretical risk that capillary damage caused by microbubbles being destroyed by ultrasound may induce neovascularization .[114] The undesirable effects that have been associated with SonoVue, the most commonly used microbubble in the UK, were in general, non-serious, transient and resolved spontaneously without residual effects. In clinical trials, the most frequently reported adverse reactions were headache (2.3%), injection site pain (1.4%), and injection site bruising, burning and paraesthesia (1.7%).66 Fatal adverse events (AEs) have occurred following the administration of microbubbles.[115,116] In the case of SonoVue, approximately 160,000 doses have been administered and 3 deaths have been temporally related, although causal relationship was uncertain. In our study, we encountered no adverse events.

CTA in the evaluation of carotid arteries

The use of CT in assessing carotid artery stenosis has increased steadily, especially with the development of multislice helical CT scanners that enable fast and accurate vessel imaging with minimal discomfort by peripheral injection of a contrast agent. High-resolution images of the luminal volume of arteries can be imaged from the aortic arch to the circle of Willis. Luminal assessment of locations of severe stenosis may be obscured with extensive plaque calcification, especially when it is circumferential. Overall, though, the sensitivity and specificity of CT angiography for carotid artery stenosis are similar to those of DSA.[117] Limitations of CT angiography include ionizing radiation doses and ballooning artifacts of heavy calcification. A recent study demonstrated the feasibility of using dual-source CT compared with histopathologic specimens after CEA to evaluate carotid plaque composition.[118]

MR plaque imaging

The development of high-resolution MRI has emerged as one of the most promising techniques for evaluating carotid atherosclerosis in vivo. A large number of studies have been conducted on human carotid arteries as they are large, superficial and suitable for imaging. MRI can be used to assess the arterial lumen as well as the wall. Noninvasive MR imaging has great potential to enable assessment of plaque burden/volume and characterization of atherosclerotic plaque composition and morphology and thus to help assess plaque vulnerability. MR imaging is well suited for plaque imaging because it is noninvasive, does not involve ionizing radiation, enables visualization of the vessel lumen and wall, and can be repeated serially to track progression or regression. By helping identify patients with unstable carotid plaques, this MR imaging technique has the potential to improve selection of patients with carotid stenosis for carotid

intervention.[67] Due to the excellent contrast resolution, carotid plaque components, including fibrous tissue, calcium, and lipid, can be identified using signal intensity variation from different weightings.[119] Yuan et al[51] also recommend multiple pulse sequences to fully characterize plaque morphology and composition. Black blood sequences with double inversion recovery preparatory pulses causes suppression of the signal of flowing blood. These can be T1, T2 and PD weighted. Bright blood sequences include TOF sequences.

Serial MR imaging of atherosclerotic plaques can provide useful insights on the natural history of vulnerable plaques and might be useful in identifying plaques that are progressing toward a vulnerable state.[92] However, it is not possible to measure the precise thickness of the fibrous cap. High-resolution MRI has been used to assess the effect of lipid-lowering treatment on carotid plaque composition.[120]

Intraplaque hemorrhage could lead to increase in plaque burden, in addition to being a reflection of the overall biological activity of the lesion.[52] MRI is capable of identifying not only the presence but also the stage of intraplaque hemorrhage.[62]

Despite the success of MRI in imaging atherosclerosis, considerable room for improvement remains, making vessel wall imaging a high activity area for technological development. The main challenges of imaging with MRI include the spatial resolution of the current systems. Also, the key determinant of plaque vulnerability may not exist within a single feature but instead may represent the complex biomechanical interplay of multiple features, this is further studied by computational fluid dynamics.[75]

The increasing availability of 3-T field strength scanners is considered to be a tremendous opportunity for improved vessel wall imaging. The increase of SNR at 3T

can be used to increase resolution and/or reduce imaging time. Experimentally, the achievable SNR improvement in carotid imaging was found to be 1.5 to 1.8 times, depending on sequence type.[121]

The other techniques for detecting plaque inflammation include thermography (measurement of plaque temperature), contrast-enhanced (CE) MRI,fluorodeoxyglucose positron emission tomography and immunoscintigraphy.[3]

Limitations

We realize that it is a limitation of our study that we do not have a gold standard (eg, histological specimens). Unfortunately, correlation with histological results is troublesome, because only patients with severe stenosis (NASCET >70% stenosis) are eligible for intervention (surgery) and have specimen available for analysis. Histopathological analysis requires special stains and immunohistochemical markers. Matching the histopathological and imaging sections is also difficult.

We did not correlate the plaque composition with patients' symptoms because of the limited sample size. As our institute is a tertiary referral center for patients with stroke, most of the patients were symptomatic. Quantitative analysis of the various components of the plaque on MRI and CTA was also not performed due to lack of availability of software.

Conclusions

We have performed a prospective study on the evaluation of carotid plaques beyond the degree of stenosis. Different modalities of imaging provide supplementary information for the characterization of carotid plaques. The echogenicity of plaques on B mode ultrasound is the basic technique for characterizing plaques. Contrast enhanced ultrasound, apart from better characterization of the stenosis and surface characteristics, can also depict the plaque neovascularization. Because CEUS agents are safe and commercially available, they can be used in the clinical setting to help in risk stratification of carotid atherosclerotic disease. CTA is a non invasive technique for evaluation of luminal stenosis which is not operator dependent, unlike ultrasound. It can also provide information about the composition of plaque based on attenuation and also the surface ulceration. It is the 'gold standard' for detecting calcification of plaques. Plaque composition, and thus vulnerability, can also be studied by MRI. Together, all these techniques provide complete information about the plaque characteristics and may be considered in planning further management of patients with carotid atherosclerotic plaques.

References

1. Warlow C, Sudlow C, Dennis M, Wardlaw J, Sandercock P. Stroke. Lancet. 2003;362:1211–1224
2. Mann JM, Davies MJ. Vulnerable plaque. Relation of characteristics to degree of stenosis in human coronary arteries. Circulation 1996;94:928-31
3. Naghavi M, Libby P, Falk E, et al. From vulnerable plaque to vulnerable patient: a call for new definitions and risk assessment strategies—part I. Circulation 2003;108: 1664–1672.
4. Naghavi M, Libby P, Falk E, et al. From vulnerable plaque to vulnerable patient: a call for new definitions and risk assessment strategies—part II. Circulation 2003;108: 1772–1778
5. Golledge J, Greenhalgh RM, Davies AH. The Symptomatic Carotid Plaque. Stroke. 2000;31:774-781
6. Marcus HS, Thomson ND, Brown MM. Asymptomatic cerebral embolic signals in symptomatic and asymptomatic carotid artery disease. Brain. 1995;118:1005–1011
7. Redgrave JN, Lovett JK, Gallagher PJ, Rothwell PM. Histological assessment of 526 symptomatic carotid plaques in relation to the nature and timing of ischemic symptoms: the Oxford plaque study. Circulation. 2006;113:2320 –2328
8. Staub D, Schinkel A, Coll B, et al. Contrast-Enhanced Ultrasound Imaging of the Vasa Vasorum From Early Atherosclerosis to the Identification of Unstable Plaques. JACC 2010;3(10) 7 6 1 – 7 1
9. Mulligan-Kehoe MJ. The vasa vasorum in diseased and nondiseased arteries. Am J Physiol Heart Circ Physiol 298: H295–H305, 2010.

10. Feinstein SB. Contrast ultrasound imaging of the carotid artery vasa vasorum and atherosclerotic plaque neovascularization. J Am Coll Cardiol 2006; 48: 236–243.
11. Carlier S, Kakadiaris IA, Dib N, et al. Vasa vasorum imaging: a new window to the clinical detection of vulnerable atherosclerotic plaques. Curr Atheroscler Rep 2005;7:164 –9.
12. Drinane M, Mollmark J, Zagorchev L, Moodie K, Sun B, Hall A, Shipman S, Morganelli P, Simons M, Mulligan-Kehoe MJ. The antiangiogenic activity of rPAI-1(23) inhibits vasa vasorum and growth of atherosclerotic plaque. Circ Res 104: 337–345, 2009.
13. Khurana R, Zhuang Z, Bhardwaj S, Murakami M, De Muinck E, Yla-Herttuala S, Ferrara N, Martin JF, Zachary I, Simons M. Angiogenesis- dependent and independent phases of intimal hyperplasia. Circulation 110: 2436–2443, 2004.
14. Langheinrich AC, Michniewicz A, Bohle RM, Ritman EL. Vasa vasorum neovascularization and lesion distribution among different vascular beds in ApoE_/_/LDL_/_ double knockout mice. Atherosclerosis 191: 73–81, 2007.
15. Moreno PR, Purushothaman KR, Fuster V, et al. Plaque neovascularization is increased in ruptured atherosclerotic lesions of human aorta: implications for plaque vulnerability. Circulation 2004;110:2032–8.
16. Fleiner M, Kummer M, Mirlacher M, et al. Arterial neovascularization and inflammation in vulnerable patients. Early and late signs of symptomatic atherosclerosis. Circulation 2004;110:2843–50.
17. McCarthy MJ, Loftus IM, Thompson MM, et al. Angiogenesis andbthe atherosclerotic carotid plaque: an association between symptomatology and plaque morphology. J Vasc Surg 1999;30:261– 8.

18. Dunmore BJ, McCarthy MJ, Naylor AR, Brindle NP. Carotid plaque instability and ischemic symptoms are linked to immaturity of microvessels within plaques. J Vasc Surg 2007;45(1):155–159.
19. Mofidi R, Crotty TB, McCarthy P, Sheehan SJ, Mehigan D, Keaveny T. Association between plaque instability, angiogenesis and symptomatic carotid occlusive disease. Br J Surg 2001;88: 945-50.
20. Homburg PJ, Rozie S, van Gils MJ, et al. Atherosclerotic plaque ulceration in the symptomatic internal carotid artery is associated with nonlacunar ischemic stroke. Stroke 2010; 41:1151–1156
21. Saba L, Montisci R, Sanfilippo R, Mallarini G. Multidetector row CT of the brain and carotid artery: a correlative analysis. Clin Radiol 2009; 64:767–778
22. Lovett JK, Rothwell PM. Site of carotid plaque ulceration in relation to direction of blood flow: an angiographic and pathological study. Cerebrovasc Dis. 2003;16:369 –375
23. Eliasziw M, Streifler JY, Fox AJ, Hachinski VC, Ferguson GG, Barnett HJ. Significance of plaque ulceration in symptomatic patients with high-grade carotid stenosis. North American Symptomatic Carotid Endarterectomy Trial. Stroke. 1994;25:304 –308.
24. Streifler JY, Eliasziw M, Fox AJ, Benavente OR, Hachinski VC, Ferguson GG, Barnett HJ. Angiographic detection of carotid plaque ulceration. Comparison with surgical observations in a multicenter study. North American Symptomatic Carotid Endarterectomy Trial. Stroke. 1994;25:1130 –1132.
25. Oliver TB, Lammie GA, Wright AR, Wardlaw J, Patel SG, Peek R, Ruckley CV, Collie DA. Atherosclerotic plaque at the carotid bifurcation: CT angiographic

appearance with histopathologic correlation. AJNR Am J Neuroradiol. 1999;20:897–901.

26. Randoux B, Marro B, Koskas F, Duyme M, Sahel M, Zouaoui A, Marsault C. Carotid artery stenosis: prospective comparison of CT, threedimensional gadolinium-enhanced MR, and conventional angiography. Radiology. 2001;220:179 –185.
27. Saba L, Caddeo G, Sanfilippo R, Montisci R, Mallarini G. Efficacy and sensitivity of axial scans and different reconstruction methods in the studyof the ulcerated carotid plaque using multidetector-row CT angiography: comparison with surgical results. AJNR Am J Neuroradiol. 2007;28: 716–723
28. Lovett JK, Gallagher PJ, Hands LJ, Walton J, Rothwell PM. Histological correlates of carotid plaque surface morphology on lumen contrast imaging. Circulation. 2004;110:2190 –2197.
29. Saba L, Sanfilipo R, Sannia S, et al. Association Between Carotid Artery Plaque Volume, Composition, and Ulceration: A Retrospective Assessment With MDCT. AJNR 2012; 199:151–156
30. Homburg PJ, Rozie S, van Gils MJ, et al. Association between carotid artery plaque ulceration and plaque composition evaluated with multidetector CT angiography. Stroke 2011; 42:367–372
31. deWeert TT, Cretier S, Groen HC, et al. Atherosclerotic Plaque Surface Morphology in the Carotid Bifurcation Assessed With Multidetector Computed Tomography Angiography. Stroke. 2009;40:1334-1340.
32. Gronholdt ML, Nordestgaard BG, Schroeder TV, Vorstrup S, Sillesen H. Ultrasonic echolucent carotid plaques predict future strokes. Circulation 2001;104(1):68e73.

33. Polak JF, Shemanski L, O'Leary DH, Lefkowitz D, Price TR, Savage PJ, et al. Hypoechoic plaque at US of the carotid artery: an independent risk factor for incident stroke in adults aged 65 years or older. Cardiovascular health study. Radiology 1998; 208(3):649-54.
34. Biasi GM, Froio A, Diethrich EB, Deleo G, Galimberti S, Mingazzini P, et al. Carotid plaque echolucency increases the risk of stroke in carotid stenting: the Imaging in Carotid Angioplasty and Risk of Stroke (ICAROS) study. Circulation 2004; 110(6):756e62.
35. Reiter M, Bucek RA, Effenberger I, Boltuch J, Lang W, Ahmadi R, et al. Plaque echolucency is not associated with the risk of stroke in carotid stenting. Stroke 2006;37(9):2378-80.
36. van Swijndregt ADM. An in-vitro evaluation of the line pattern of the near and far walls of carotid arteries using B-mode ultrasound. Ultrasound Med Biol 1996;22:1007–15.
37. Wong M, Edelstein J, Wollman J, Bond MG. Ultrasonic-pathological comparison of the human arterial wall. Verification of intima-media thickness. Arterioscler Thromb 1993;13:482– 6.
38. Coli S, Magnoni M, Sangiorgi G, et al. Contrast-Enhanced Ultrasound Imaging of Intraplaque Neovascularization in Carotid Arteries Correlation With Histology and Plaque Echogenicity. JACC 2008; 52(3): 223-30
39. Shah F, Balan P, Weinberg M, Reddy V, Neems R, Feinstein M, et al. Contrast-enhanced ultrasound imaging of atherosclerotic carotid plaque neovascularisation: a new surrogate marker of atherosclerosis? Vasc Med 2007;12:291-8.

40. Giannoni MF, Vicenzini E, Citone M, Ricciardi MC, Irace L, Laurito A, et al. Contrast carotid ultrasound for the detection of unstable plaques with neoangiogenesis: a pilot study. Eur J Vasc Endovasc Surg 2009;37(6):722-7.
41. Fagglioli GL, Pini R, Mauro R et al. Identification of Carotid 'Vulnerable Plaque' by Contrast-enhanced Ultrasonography: Correlation with Plaque Histology, Symptoms and Cerebral Computed Tomography. Eur J Vasc Endovasc Surg (2011) 41, 238-248
42. Xiong L, Deng YB, Zhu Y, Liu YN, Bi XJ. Correlation of carotid plaque neovascularization detected by using contrast-enhanced US with clinical symptoms. Radiology 2009;251(2):583-9.
43. Hoogi A, Adam D, Hoffman A, et al. Carotid Plaque Vulnerability: Quantification of Neovascularization on Contrast-Enhanced Ultrasound With Histopathologic Correlation AJR 2011; 196:431–436
44. Moreno PR, Fuster V. New aspects in the pathogenesis of diabetic atherothrombosis. J Am Coll Cardiol 2004;44:2293–300.
45. Mauriello A, Sangiorgi G, Fratoni S, et al. Diffuse and active inflammation occurs in both vulnerable and stable plaques of the entire coronary tree: a histopathologic study of patients dying of acute myocardial infarction. J Am Coll Cardiol 2005;45:1585–93.
46. Owen DR, Shalhoub J, Miller S, et al. Inflammation within Carotid Atherosclerotic Plaque: Assessment with Late-Phase Contrast-enhanced US. Radiology 2010;255(2):638-44
47. Williams JK, Armstrong ML, Heistad DD. Vasa vasorum in atherosclerotic coronary arteries: responses to vasoactive stimuli and regression of atherosclerosis. Circ Res 1988;62:515–23.

48. Moulton KS, Vakili K, Zurakowski D, et al. Inhibition of plaque neovascularization reduces macrophage accumulation and progression of advanced atherosclerosis. Proc Natl Acad Sci U S A 2003;100: 4736–41.
49. Cosgrove D. Ultrasound contrast agents: an overview. Eur JRadiol 2006;60(3):324-30
50. Shalhoub J, Owen DRJ, Gauthier T, et al. The use of Contrast Enhanced Ultrasound in Carotid Arterial Disease Eur J Vasc Endovasc Surg (2010) 39, 381-387
51. Yuan C, Mitsumori LM, Ferguson MS, et al. In vivo accuracy of multispectral magnetic resonance imaging for identifying lipid-rich necrotic cores and intraplaque hemorrhage in advanced human carotid plaques. Circulation 2001;104:2051–2056
52. Virmani R, Kolodgie FD, Burke AP, Farb A, Schwartz SM. Lessons from sudden coronary death: a comprehensive morphological classification scheme for atherosclerotic lesions. Arterioscler Thromb Vasc Biol 2000;20:1262–1275
53. Yuan C, Zhang SX, Polissar NL, Echelard D, Ortiz G, Davis JW et al. Identification of fibrous cap rupture with magnetic resonance imaging is highly associated with recent transient ischemic attack or stroke. Circulation 2002;105:181–185
54. Shinnar M, Fallon JT, Wehrli S, et al. The diagnostic accuracy of ex vivo MRI for human atherosclerotic plaque characterization. Arterioscler Thromb Vasc Biol 1999; 19:2756–2761
55. Yuan C, Mitsumori LM, Beach KW, Maravilla KR. Carotid Atherosclerotic Plaque: Noninvasive MR Characterization and Identification of Vulnerable Lesions. Radiology 2001; 221:285–299

56. Cai JM, Hatsukami TS, Ferguson MS, Small R, Polissar NL, Yuan C. Classification of human carotid atherosclerotic lesions with in vivo multicontrast magnetic resonance imaging. Circulation 2002;106:1368–1373
57. Clarke SE, Hammond RR, Mitchell JR, Rutt BK. Quantitative assessment of carotid plaque composition using multicontrast MRI and registered histology. Magn Reson Med 2003;50:1199–1208.
58. Saam T, Ferguson MS, Yarnykh VL, et al. Quantitative evaluation of carotid plaque composition by in vivo MRI. Arterioscler Thromb Vasc Biol 2005;25:234–239.
59. Cai J, Hatsukami TS, Ferguson MS, et al. In Vivo Quantitative Measurement of Intact Fibrous Cap and Lipid-Rich Necrotic Core Size in Atherosclerotic Carotid Plaque Comparison of High-Resolution, Contrast-Enhanced Magnetic Resonance Imaging and Histology. Circulation. 2005;112:3437-3444
60. Sakamoto M, Taoka, T, Nakagawa H, et al. Magnetic resonance plaque imaging to predict the occurrence of the slow-flow phenomenon in carotid artery stenting procedures Neuroradiology (2010) 52:275–283
61. Yuan C, Mitsumori LM, Ferguson MS, Polissar NL, Echelard D, Ortiz G, Small R, Davies JW, Kerwin WS, Hatsukami TS. In vivo accuracy of multispectral magnetic resonance imaging for identifying lipid-rich necrotic cores and intraplaque hemorrhage in advanced human carotid plaques. Circulation. 2001;104:2051–2056.
62. Chu B, Kampschulte A, Ferguson MS, et al. Hemorrhage in the Atherosclerotic Carotid Plaque: A High-Resolution MRI Study. Stroke. 2004;35:1079-1084
63. Kampschulte A, Ferguson MS, Kerwin WS, et al. Differentiation of Intraplaque Versus Juxtaluminal Hemorrhage/Thrombus in Advanced Human Carotid

Atherosclerotic Lesions by In Vivo Magnetic Resonance Imaging. Circulation. 2004;110:3239-3244

64. Ota H, Yarnykh VL, Ferguson MS et al. Carotid Intraplaque Hemorrhage Imaging at 3.0-T MR Imaging: Comparison of the Diagnostic Performance of Three T1-weighted Sequences Radiology2010: 254(2) 551-63
65. Murphy RE, Moody AR, Morgan PS, Martel AL, Delay GS, Allder S, MacSweeney ST, Tennant WG, Gladman J, Lowe J, Hunt BJ. Prevalence of complicated carotid atheroma as detected by magnetic resonance direct thrombus imaging in patients with suspected carotid artery stenosis and previous acute cerebral ischemia. Circulation. 2003;107:3053–3058.
66. Altaf N, Beech A , Goode SD , et al . Carotid intraplaque hemorrhage detected by magnetic resonance imaging predicts embolization during carotid endarterectomy . J Vasc Surg 2007 ; 46 (1): 31 – 36 .
67. Altaf N, Goode SD, Beech A, et al. Plaque Hemorrhage Is a Marker of Thromboembolic Activity in Patients with Symptomatic Carotid Disease. Radiology 2011; 258(2): 538-45
68. Hatsukami TS, Ross R, Polissar NL, Yuan C. Visualization of fibrous cap thickness and rupture in human atherosclerotic carotid plaque in vivo with high-resolution magnetic resonance imaging. Circulation 2000;102:959–964.
69. Mitsumori LM, Hatsukami TS, Ferguson MS, Kerwin WS, Cai J, Yuan C. In vivo accuracy of multisequence MR imaging for identifying unstable fibrous caps in advanced human carotid plaques. J Magn Reson Imaging 2003;17:410–420.
70. Touze E, Toussaint JF, Coste J, et al. Reproducibility of high-resolution MRI for the identification and the quantification of carotid atherosclerotic plaque

components: consequences for prognosis studies and therapeutic trials. Stroke 2007;38: 1812–1819.

71. Raman SV, Winner MW 3rd, Tran T, et al. In vivo atherosclerotic plaque characterization using magnetic susceptibility distinguishes symptom-producing plaques. JACC Cardiovasc Imaging. 2008;1:49-57.
72. Zhu DC, Ota H, Vu AT, et al. An optimized 3D spoiled gradient for hemorrhage assessment using inversion recovery and multiple echoes (3D SHINE) for carotid plaque imaging. Paper presented at: the 17th International Society of Magnetic Resonance in Medicine Meeting. April 17Y24, 2009; Honolulu, HI; p. 606.
73. Yang Q, Liu J, Barnes SR, et al. Imaging the vessel wall in major peripheral arteries using susceptibility-weighted imaging. J Magn Reson Imaging. 2009;30:357Y365.
74. Gatehouse PD, Bydder GM. Magnetic resonance imaging of short T2 components in tissue. Clin Radiol. 2003;58:1Y19.
75. Kerwin WS, Canton G. Advanced Techniques for MRI of Atherosclerotic Plaque. Top Magn Reson Imaging 2009; 20(4): 217-225
76. Toussaint JF, Southern JF, Fuster V, et al. Water diffusion properties of human atherosclerosis and thrombosis measured by pulse field gradient nuclear magnetic resonance. Arterioscler Thromb Vasc Biol. 1997;17:542-546.
77. Clarke SE, Hammond RR, Mitchell JR, et al. Quantitative assessment of carotid plaque composition using multicontrast MRI and registered histology. Magn Reson Med. 2003;50:1199-1208.
78. Kerwin WS, Oikawa M, Yuan C, et al. MR imaging of adventitial vasa vasorum in carotid atherosclerosis. Magn Reson Med. 2008;59:507Y514.

79. Saam T, Yuan C, Chu B, et al. Predictors of carotid atherosclerotic plaque progression as measured by noninvasive magnetic resonance imaging. Atherosclerosis 2007;194(2):e34-42.
80. Corti R, Fayad Z, Fuster V, et al. Effects of lipid lowering by simvastatin on human atherosclerotic lesions: a longitudinal study by high-resolution, noninvasive magnetic resonance imaging. Circulation 2001;104:249–252.
81. Wasserman BA, Smith WI, Trout HH 3rd, Cannon RO 3rd, Balaban RS, Arai AE. Carotid artery atherosclerosis: in vivo morphologic characterization with gadolinium-enhanced doubleoblique MR imaging—initial results. Radiology 2002;223:566–573.
82. Trivedi RA, U-King-Im JM, Graves MJ, et al. In vivo detection of macrophages in human carotid atheroma: temporal dependence of ultrasmall superparamagnetic particles of iron oxide-enhanced MRI. Stroke 2004;35:1631–1635.
83. Sitzer M, Muller W, Siebler M, et al. Plaque ulceration and lumen thrombus are the main sources of cerebral microemboli in high-grade internal carotid artery stenosis. Stroke 1995;26:1231-3
84. Schroeder S, Kopp AF, Baumbach A, et al. Noninvasive detection and evaluation of the atherosclerotic plaque with multislice computed tomography. J Am Coll Cardiol 2001; 37:1430-5.
85. Weinberger J. Diagnosis and prevention of atherosclerotic cerebral infarction. CNS Spectr 2005;10:553–564
86. Beneficial effect of carotid endarterectomy in symptomatic patients with high-grade carotid stenosis. North American Symptomatic Carotid Endarterectomy Trial Collaborators. N Engl J Med 325:445-453, 1991

87. MRC European Carotid Surgery Trial: Interim results for symptomatic patients with severe (70-99%) or with mild (0-29%) carotid stenosis. European Carotid Surgery Trialists' Collaborative Group. Lancet 337: 1235-1243, 1991
88. Executive Committee for the Asymptomatic Carotid Atherosclerosis Study. Endarterectomy for asymptomatic carotid artery stenosis. *JAMA*. 1995;273:1421–1428.
89. MRC Asymptomatic Carotid Surgery Trial (ACST) Collaborative Group. Prevention of disabling and fatal strokes by successful carotid endarterectomy in patients without recent neurological symptoms: randomized controlled trial. Lancet 2004;363(9420):1491–502
90. Saam T, Cai J, Ma L, Cai Y, Ferguson M, Polissar N et al. Comparison of symptomatic and asymptomatic atherosclerotic carotid plaque features with in vivo MR imaging. Radiology 2006;240:464–472
91. Glagov S, Weisenberg E, Zarins CK, et al. Compensatory enlargement of human atherosclerotic coronary arteries. N Engl J Med. 1987;316:1371Y1375.
92. Glagov S, Zarins C, Giddens DP, Ku DN: Hemodynamics and atherosclerosis. Insights and perspectives gained from studies of human arteries. Arch Pathol Lab Med 1988, 112:1018–1031.
93. Lee D, Chiu JJ: Intimal thickening under shear in a carotid bifurcation—a numerical study. J Biomech 1996, 29:1–11.
94. Yazdani SK, Vorpahl M, Ladich E, et al. Pathology and Vulnerability of Atherosclerotic Plaque: Identification, Treatment Options, and Individual Patient Differences for Prevention of Stroke. Current Treatment Options in Cardiovascular Medicine (2010) 12:297–314

95. Chakfé N, Durand B, Kretz JG (eds): New Technologies in Vascular Biomaterials: Fundamentals About Stents II. Strasbourg, France: EUROPROT; 2007

96. Mauriello A, Sangiorgi GM, Virmani R, et al.: A pathobiologic link between risk factors profile and morphological markers of carotid instability. Atherosclerosis 2009, 208:572–580.

97. Avril G, Batt M, Guidoin R, et al.: Carotid endarterectomy plaques: correlations of clinical and anatomic findings. Ann Vasc Surg 1991, 5:50–54.

98. Golledge J, Greenhalgh RM and Davies AH. The Symptomatic Carotid Plaque Stroke.2000;31:774-781

99. Kullo IJ, Edwards WD, Schwartz RS. Vulnerable plaque: pathobiology andclinical implications.Ann InternMed1998;129:1050e60.

100. Kolodgie FD, Burke AP, Farb A, Gold HK, Yuan J, Narula J, et al. The thin-cap fibroatheroma: a type of vulnerable plaque: the major precursor lesion to acute coronary syndromes. Curr Opin Cardiol 2001;16:285e92.

101. Doherty TM, Fitzpatrick LA, Inoue D, Qiao JH, Fishbein MC, Detrano RC, et al. Molecular, endocrine, and genetic mechanisms of arterial calcification. Endocr Rev 2004;25(4): 629-72.

102. Spagnoli LG, Bonanno E, Sangiorgi G, Mauriello A. Role of inflammation in atherosclerosis. J Nucl Med 2007;48(11): 1800-15.

103. Schonbeck U, Mach F, Sukhova GK, Murphy C, Bonnefoy JY, Fabunmi RP, Libby P. Regulation of matrix metalloproteinase expression in human vascular smooth muscle cells by T lymphocytes. *Circ Res*. 1997;81: 448–454.

104. Köester W. Endarteriitis and arteriitis. Berl Klin Wochenschr 1876; 12:454 –5.

105. Winternitz MC, Thomas RM, LeCompte PM. The Biology of Arteriosclerosis. Springfield, IL: Charles C Thomas, 1938.

106. Grant EG, Benson CB, Moneta GL, Alexandrov AV, Baker JD, Bluth EI, et al. Carotid artery stenosis: gray-scale and Doppler US diagnosis society of radiologists in ultrasound consensus conference. Radiology 2003;229(2):340-6.

107. Sidhu PS, Allan PL. Ultrasound assessment of internal carotid artery stenosis. Clin Radiol 1997;52(9):654-8.

108. Filis KA, Arko FR, Johnson BL, Pipinos II, Harris EJ, Olcott Ct, et al. Duplex ultrasound criteria for defining the severity of carotid stenosis. Ann Vasc Surg 2002;16(4):413-21.

109. Oates CP, Naylor AR, Hartshorne T, Charles SM, Fail T, Humphries K, et al. Joint recommendations for reporting carotid ultrasound investigations in the United Kingdom. Eur J Vasc Endovasc Surg 2009;37(3):251-61.

110. Halliday A, Mansfield A, Marro J, Peto C, Peto R, Potter J, et al. Prevention of disabling and fatal strokes by successful carotid endarterectomy in patients without recent neurological symptoms: randomised controlled trial. Lancet 2004;363(9420): 1491-502.

111. McCarthy MJ, Loftus IM, Thompson MM, Jones L, London NJM, Bell PRF, et al. Angiogenesis and the atherosclerotic carotid plaque: an association between symptomatology and plaquemorphology. J Vasc Surg 1999;30:261-8.

112. Milei J, Parodi JC, Jose´ Alonso GF, Barone A, Grana D, Matturri L. Carotid rupture and intraplaque haemorrhage: immunophenotype and role of cells involved. Am Heart J 1998; 136:1096-105.

113. Kockx M, Cromheeke KM, Knaapen M, Bosmans JM, DeMeyer GRY, Herman AG, et al. Phagocytosis and macrophage activation associated with

hemorrhagic microvessels in human atherosclerosis. Arterioscler Thromb Vasc Biol 2003;23:440-6.

114. Yoshida J, Ohmori K, Takeuchi H, Shinomiya K, Namba T, Kondo I, et al. Treatment of ischemic limbs based on local recruitment of vascular endothelial growth factor-producing inflammatory cells with ultrasonic microbubble destruction. J Am Coll Cardiol 2005;46(5):899-905.

115. Bracco. SonoVue. Summary of product characteristics. In; 2005.

116. Dijkmans PA, Visser CA, Kamp O. Adverse reactions to ultrasound contrast agents: is the risk worth the benefit? Eur J Echocardiogr 2005;6(5):363-6.

117. Anderson GB, Ashforth R, Steinke DE, et al.: CT angiography for the detection and characterization of carotid artery bifurcation disease. Stroke 2000, 31:2168–2174.

118. Das M, Braunschweig T, Muhlenbruch G, et al.: Carotid plaque analysis: comparison of dual-source computed tomography (CT) findings and histopathological correlation. Eur J Vasc Endovasc Surg 2009, 38:14–19

119. Zhao XQ, Yuan C, Hatsukami TS, et al.: Effects of prolonged intensive lipid-lowering therapy on the characteristics of carotid atherosclerotic plaques in vivo by MRI: a case-control study. Arterioscler Thromb Vasc Biol 2001, 21:1623–1629.

120. Shinnar M, Fallon JT, Wehrli S, et al.: The diagnostic accuracy of ex vivo MRI for human atherosclerotic plaque characterization. Arterioscler Thromb Vasc Biol 1999, 19:2756–2761

121. Yarnykh VL, Terashima M, Hayes CE, et al. Multicontrast black-blood MRI of carotid arteries: comparison between 1.5 and 3 tesla magnetic field strengths. J Magn Reson Imaging. 2006;23:691-698.

Annexures

Proforma

- **Patient history and clinical details**
    - Patient demographics (age, gender)
    - History of chief complaints (Transient ischemic attack, stroke, number of episodes, time since last ictus)
    - Risk factors (smoking, diabetes mellitus, hypertension, coronary artery disease)
- **Ultrasound findings**
    - Presence of plaque
    - Stenosis according to NASCET criteria
    - Plaque echogenicity
    - Contrast enhancement and neovascularity
    - Plaque surface – regular / irregular / ulcerated
- **MRI findings**
    - Signal intensity on
        - T1 dark blood fat saturated
        - T2 dark blood fat saturated
        - PD dark blood fat saturated
        - MRA TOF source images
    - Fibrous cap and ukceration
- **CT angiography findings**
    - Degree of stenosis
    - Pre-contrast attenuation (Hounsfield units) – uniform / non-uniform
    - Degree of contrast enhancement in Hounsfield units
    - Distribution of contrast enhancement – uniform / non-uniform, peripheral / central

Technical Advisory Committee (Clinical Studies)

SREE CHITRA TIRUNAL INSTITUTE FOR MEDICAL SCIENCE & TECHNOLOGY
THIRUVANANTHAPURAM – 695011, INDIA

TAC Registration No: SCT-/S/2010/52 **Date: 20.01.2011**

Project title: Multimodality Plaque Imaging: Comparison of contrast enhanced USG, CT and MRI

Principal Investigator:
NAME: Dr. Divyata Rajendra Hingwala Degree: MD Address: DM Neuroradiology Resident, Department of Imaging science and Interventional Radiology, SCTIMST, Thiruvananthapuram, Kerala, India. PIN: 695011
Co-Principal Investigator(s)
(1) NAME: Dr. Chandrasekharan Kesavadas Degree: MD, DMRD Address: Additional Professor, Department of Imaging science and Interventional Radiology, SCTIMST, Thiruvananthapuram, Kerala, India. PIN: 695011
(2) NAME: Dr. Bejoy Thomas Degree: MD, DNB, PDCC Address: Additional Professor, Department of Imaging science and Interventional Radiology, SCTIMST, Thiruvananthapuram, Kerala, India. PIN: 695011
(3) NAME: Dr. Hima S. Pendharkar Degree: DMRD, DNB, DM Neuroradiology Address: Assistant Professor, Department of Imaging science and Interventional Radiology, SCTIMST,Thiruvananthapuram, Kerala, India. PIN: 695011
(4) NAME: Dr. Sylaja P N Degree: MD, DM NEUROLOGY Address: Additional Professor, Department of Neurology, SCTIMST, THIRUVANANTHAPURAM, KERALA, INDIA. PIN: 695011
(5) NAME: Dr. M Unnikrishnan Degree: MS, MCH CVTS, FIACS ADDRESS: Professor, Department of Cardiovascular and Thoracic Surgery, SCTIMST, THIRUVANANTHAPURAM, KERALA, INDIA. PIN: 695011
(6) NAME: Dr. T R Kapilamoorthy Degree: DMRD, MD, PDCC Address: Additional Professor, Department of Imaging science and Interventional Radiology, SCTIMST,, Thiruvananthapuram, Kerala, India. PIN: 695011

Members who participated in the TAC meeting on 11-1-2011
Dr. V. Mohan Kumar (Chairman)
Dr. R. Sankar Kumar
Dr. Narayanan Namboodiri
Dr. K. Shivakumar (Member Secretary)

Members who participated in the TAC meeting on 18-1-2011
Dr. V. Mohan Kumar (Chairman)
Dr. R. Sankar Kumar
Dr. K. Srinivasan
Dr. T. V. Kumary
Dr. Narayanan Namboodiri
Dr. K. Shivakumar (Member Secretary)

Risk Classification of the project (Minimum/ Moderate/ High): Moderate

Requirement of DSMB: No

Recommended members of DSMB: Not applicable

Recommendations of TAC:

Recommended for consideration of IEC in the light of the responses received from the investigator.

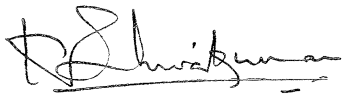

Signature of the Member Secretary, TAC (Clinical Studies)

Note for IEC
Copy of the investigator's responses to questions/suggestions from TAC is attached (Appendix-1).

श्री चित्रा तिरुनाल आयुर्विज्ञान और प्रौघोगिकी संस्थान
तिरुवनन्तपुरम - 695 011, केरल, इंडिया
SREE CHITRA TIRUNAL INSTITUTE FOR MEDICAL SCIENCES AND TECHNOLOGY
THIRUVANANTHAPURAM - 695 011, INDIA
(An Institute of National Importance under Govt. of India)

Institutional Ethics Committee (IEC)

SCT / IEC-324/ MAY-2011

08-06-2011

Dr. Divyata Rajendra Hingwala
DM Neuroradiology Resident
Department of ISIR
SCTIMST

Dear Dr. Divyata Rajendra Hingwala,

The Institutional Ethics Committee reviewed and discussed your application to conduct the clinical trial entitled "Multimodality Plaque Imaging: Comparison of Contrast Enhanced USG, CT and MRI"/IEC 324".

The following documents were reviewed:

1. Covering letter dated 30-04-2011.

तार : चित्रमेट फोन फाक्स ई-मेइल
Grams : Chitramet Phone : 2443152 Fax : (91) 471 - 2446433 2550728 E-mail : sct.@sctimst.ker.nic.in

IEC Decision

IEC noted the documents and approved.

Remarks:

The Institutional Ethics Committee expects to be informed about the progress of the study, any SAE occurring in the course of the study, any changes in the protocol and patient information/informed consent and asks to be provided a copy of the final report.

There was no member of the study team who participated in voting / decision making process. The ethics committee is organized and operated according to the requirements of Good Clinical Practice and the requirements of the Indian Council of Medical Research (ICMR).

Yours Sincerely

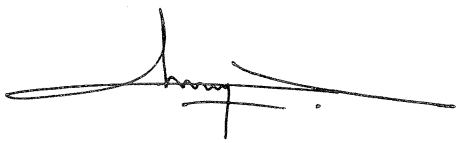

Dr. Anoopkumar Thekkuveettil
Member Secretary, Ethics Committee.

श्री चित्रा तिरुनाल आयुर्विज्ञान और प्रौद्योगिकी संस्थान
तिरुवनन्तपुरम - 695 011, केरल, इंडिया
SREE CHITRA TIRUNAL INSTITUTE FOR MEDICAL SCIENCES AND TECHNOLOGY
THIRUVANANTHAPURAM - 695 011, INDIA
(An Institute of National importance under Govt. of India)

Dir/INT.PROJ/SCTISMT/2011
20.01.2011

Dr. Divyata Rajendra Hingwala
Senior Resident,
Department of IS&IR
SCTIMST, Thiruvananthapuram-11

Dear Dr. Divyata Rajendra Hingwala,

The Committee on Institute Funding for Internal Projects reviewed your project proposal titled "Multimodality Plaque Imaging: Comparison of contrast enhanced USG, CT and MRI " and we are pleased to inform you that we arrived at the collective decision to approve the project for funding. The fund allotted for this project shall be Rs.50,000/-. (Rupees Fifty Thousand only).

Funds will be released subject to IEC clearance wherever required.

All the conditions specified in the Guidelines for Institute Funding for internal projects for Faculty and Senior Residents dt. 11.03.2010 shall be adhered to. Copy of the guidelines enclosed.

Yours sincerely,

Director

तार : चित्रमेट | फोन | फाक्स | ई-मेइल
Grams : Chitramet | Phone : 2443152 | Fax : (91)471-2446433 2550728 | E-mail : sct. @sctimst.ker.nic.in

Masterchart

Sr no	age	sex	stroke	TIA	carotid	% stenosis	PD	T2	T1	TOF	composition
1	75	M	lt MCA	10	left	90	iso	hypo	mildly hyper	iso	lipid
M2	73	M	lt MCA	2	bil	45, 73	iso	hypo	hyper	hyper	lipid with recent he
3	75	M	lt MCA	2	bil	99, 50	iso	iso	mildly hyper	iso	fibrous
4	74	F	rt MCA	8	bil	75, 30	hyper	hyper	hyper	iso	blood thrombus
5	45	F	lt MCA	n	left	99	iso	iso	mildly hyper	iso	fibrous
6	65	M	n	3	left	70	iso	hypo with small hyper comp	small hyper comp	iso	fibro-fatty with small he
7	77	M	n	3	right	75	iso	iso	mildly hyper	iso	fibrous
8	60	M	n	>10	right	70	iso	hypo	mildly hyper	iso	lipid
9	72	M	rt MCA-ACA	n	bil	50, 70	iso	iso	mildly hyper	iso	fibrous
10	71	F	rt MCA	n	bil	50, 60					
11	48	M	lt MCA	n	left	60	hyper	hyper	mildly hyper	hyper	hemorrhagic
12	53	M	n	n	left	60					
13	60	M	lt ACA-MCA	n	left	99					
14	75	M	lt MCA	n	left	70	iso	iso	mildly hyper	iso	fibrous with little lipid
15	67	M	lt MCA	1	left	90	iso	hypo	mildly hyper	iso	fibro-fatty
16	66	M	rt MCA	6	bil	90, 90					
17	48	M	rt MCA ACA watershed	1	right	70	hyper	hyper	hyper	hyper	hemorrhagic
18	48	M	n	n	bil	99,99	iso	iso, hyper	iso, hyper	iso, hyper	fibrous, fibrofatty with he
19	68	M	n	1	bil	70, 72	iso	iso	mildly hyper	iso	fibrous
20	59	M	n	1	left	80	iso	iso	mildly hyper	iso	fibrofatty
21	80	M	n	4	left	80	iso	hypo	mildly hyper	iso	lipid
22	71	M	n	1	left	80	iso	hypo with small hyper comp	small hyper comp	iso	fibro-fatty with small he
23	68	M	lt MCA	n	left	90	iso	hypo	iso	Iso	fibrofatty
24	72	M	y rt	>10 left	bil	50,70					

Masterchart

Sr no	fibrous cap	ulcer	CEUS	CEUS ulc	plain	CTA atten	CTA ulc	CT calc
1	y	n			hypo	28.9	n	y
2	n	y			hyper	31	y	y
3	y	n			hyper sha	73.3	n	y
4	n	n			hyper	50.9	n	y
5	y	n			hyper	CTA outside		
6	n	y			hypo	66.1	y	n
7	n	n	n	n	hyper	61.8	n	y
8	n	n			hypo	DSA		
9	n	y	y	y	hypo	56.9	y	y
10			n	n	hypo	4.8	n	n
11	n	y	y	n	mixed	52.9	y	y
12			n	n	hypo			
13			y	n	hyper	39.7	n	y
14	y	y	n	n	hyper	CTA outside		
15	y	y	y	n	hyper sha	37.6	y	y
16			n	y	hypo	57.8	n	y
17	n	y	y	y	hyper sha	DSA		
18	y	n	n,y	n,n	hyper	MRA		
19	y	y	y	y (left)	hyper sha	79	y	y
20	y	y	n	n	hyper	43.8	n	y
21	y	y	n	n	hypo	33.1	y	y
22	n	y	y	n	mixed	37.7	y	y
23	y	n			hypo	78	n	n
24			y,y	n,n	hypo, hypo	74,39.3	n,n	n,y

Key- MRI – iso – isointense, hypo – hypointense, hyper- hyperintense, he – hemorrhage, y – present, n – absent, USG - hypo – hypoechoic, hyper – hyperechoic, hyper sha – hyperechoic with posterior acoustic shadowing, atten –attenuation, ulc – ulceration, calc - calcification